Journal of Physiology (1997), **500.3**, *pp.*751–774

Synaptic origin and stimulus dependency of neuronal oscillatory activity in the primary visual cortex of the cat

Vincent Bringuier, Yves Frégnac*, Attila Baranyi, Dominique Debanne and Daniel E. Shulz

Equipe Cognisciences, Institut Alfred Fessard, CNRS, 91198 Gif sur Yvette, France

1. We have studied the oscillatory activity of single neurons (91 recorded extracellularly and 76 intracellularly) in the primary visual cortex of cats and kittens to characterize its origins and its stimulus dependency. A new method for the detection of oscillations was developed in order to maximize the range of detectable frequencies in both types of recordings. Three types of activity were examined: spontaneous background activity, responses to intracellular current steps and visual responses.

2. During spontaneous activity, persistent oscillatory activity was very rare in both types of recordings. However, when intracellular records were made using KCl-filled micropipettes, spontaneous activity appeared rhythmic and contained repeated depolarizing events at a variety of frequencies, suggestive of tonic periodic inhibitory input normally masked at resting potential.

3. Patterns of firing activity in response to intracellular current steps allowed us to classify neurons as regular spiking, intrinsically bursting, and fast-spiking types, as described *in vitro*. In the case of rhythmically firing cells, the spike frequency increased with the amount of injected current. Subthreshold current-induced oscillations were rarely observed (2 out of 76 cells).

4. Visual stimulation elicited oscillations in one-third of the neurons (55 out of 167), predominantly in the 7–20 Hz frequency range in 93% of the cases. Rhythmicity was observed in both simple and complex cells, and appeared to be more prominent at 5 and 6 weeks of age.

5. Intracellular recordings in bridge mode and voltage clamp revealed that visually evoked oscillations were driven by synaptic activity and did not depend primarily on the intrinsic properties of recorded neurons. Hyperpolarizing the membrane led to an increase in the size of the rhythmic depolarizing events without a change in frequency. In voltage-clamped cells, current responses showed large oscillations at the same frequency as in bridge mode, independently of the actual value of the holding potential.

6. In fourteen intracellularly recorded neurons, oscillations consisted of excitatory events that could be superimposed on a depolarizing or a hyperpolarizing slow wave. In two other neurons, visual responses consisted of excitatory and inhibitory events, alternating with a constant phase shift.

7. Drifting bars were much more efficient in evoking oscillatory responses than flashed bars. Except in three cells, the frequency of the oscillation did not depend on the physical characteristics of the stimulus that were tested (contrast, orientation, direction, ocularity and position in the receptive field). No significant correlation was found between the intensity of the visual response and the strength of the rhythmic component.

8. Although it cannot be excluded that the dominant frequency of oscillations might be related to the type of anaesthetics used, no correlation was found between local EEG and the oscillatory activity elicited by visual stimulation.

9. We conclude that the oscillations observed in the present work are generated by synaptic activity. It is likely that they represent an important mode of transmission in sensory processing, resulting from periodic packets of synchronized activity propagated across recurrent circuits. Their relevance to perceptual binding is further discussed.

* To whom correspondence should be addressed.

Statistical analysis of the visually evoked firing of cortical cells reveals that some neurons have an oscillatory activity, i.e. they tend to emit action potentials in a periodic manner (Gray, Engel, König & Singer, 1990). This behaviour is in contrast to the dominant firing process of central neurons, usually observed in their resting mode, and characterized by a distribution of the interspike intervals of the Poisson type, where a refractory period in addition limits the occurrence of the shorter intervals (Cox, 1962). Theoretically, periodic firing could stem from pacemaker properties of the cell, or from a source of periodicity already contained in the input. Experimental evidences for these two types of mechanisms have been found in different cortical areas.

Pacemaker properties at frequencies ranging from 5 to 50 Hz are present in the subthreshold and in the spiking activity. Subthreshold oscillations have been recorded *in vitro* in stellate cells of entorhinal cortex (Alonso & Klink, 1993) and depend on a persistent sodium current. They are also present in pyramidal cells of frontal cortex where a potassium current sets their resonant frequency and a persistent sodium current controls their amplitude (Gutfreund, Yarom & Segev, 1995). Current-induced periodic firing has been reported essentially in intrinsically bursting and fast-spiking cells, since regular cells classically exhibit discharge adaptation and therefore lack endogenous rhythmicity. Recently, McCormick & Gray (1995) have described a new category of neocortical cells, termed 'chattering cells', that can emit periodic bursts at high frequencies in response to current injection.

However, periodicity can also be synaptically driven through reverberation of activity in a network of non-pacemaker neurons, as illustrated by many models, including recurrent connections, either only excitatory (Deppisch, Bauer, Schillen, König, Pawelzik & Geise, 1993) or excitatory and inhibitory (Wilson & Cowan, 1972; König & Schillen, 1991). An interplay between local excitatory and inhibitory connectivity and intrinsic voltage-dependent properties determines the spindle-like oscillations observed in slices of thalamus, where reciprocal connections between peri-geniculate and lateral geniculate nuclei are preserved (Von Krosigk, Bal & McCormick, 1993). Synaptically driven periodicity can also be inherited from extrinsic projections. For instance, it is well established that the spontaneous spindles observed during barbiturate anaesthesia are generated in the thalamus and propagated to the cortex (for review, see Andersen & Andersson, 1968). Using intracellular recording in the motor cortex, Creutzfeldt, Watanabe & Lux (1966) have observed systematic correlations between the negative peaks of the surface EEG spindles and intracellular depolarizations.

The study of oscillatory activity in the visual cortex recently regained interest because stimulus-induced neural oscillations have been shown to synchronize across large cortical distances as a function of global features of the stimulus (Eckhorn *et al.* 1988; Gray, König, Engel & Singer, 1989). The source of such visually evoked periodicity has been documented at the intracellular level by several studies. An early report, based on a small number of cells, described periodic inhibitory potentials during visual stimulation, but no quantitative analysis was performed (Ferster, 1986). The same laboratory, using blind patch-clamp recordings, later reported rhythmic potentials that were assumed to be synaptic because their frequency did not vary with polarization of the membrane potential (Jagadeesh, Gray & Ferster, 1992). However, the role of inhibitory and excitatory synaptic potentials, and the importance of these phenomena across the population of cortical cells still need to be clarified.

In the present study we developed an analysis of oscillatory behaviour in single cells based on periodicity detection in autocorrelation histograms or functions, and applied this method to extracellular and intracellular recordings in the kitten and cat visual cortex. Using intracellular injection of DC current and voltage clamp in combination with visual stimulation, we studied the origins of oscillatory behaviour at the cellular level, its stimulus dependency and its possible implication in perceptual binding.

Part of this work has been briefly presented elsewhere (Bringuier, Frégnac, Debanne, Shulz & Baranyi, 1992).

METHODS

Animals, surgical preparation and physiological controls

Normally reared kittens from our breeding colony, aged from 4 to 24 weeks of age, and adult cats (over 1 year of age) were used for this study. Initial anaesthesia was induced by intramuscular injection of Althesin (Glaxo, 1·2 ml kg^{-1}; 10·8 mg kg^{-1} alfaxalone and 3·6 mg kg^{-1} alfadolone acetate). After cannulation of the femoral vein and tracheotomy, the animal was installed in a Horsley-Clarke stereotaxic frame. Anaesthesia and muscular paralysis were maintained by a continuous intravenous infusion that contained Althesin (3 mg kg^{-1} h^{-1}) and Flaxedil (gallamine triethiodide, 15 mg kg^{-1} h^{-1}), supplemented with 0·9% glucose and NaCl. Body temperature was kept at 38 °C. Artificial respiration was maintained at 25 strokes per minute, and the volume of inhaled air adjusted to maintain the end-tidal CO_2 concentration between 3·8 and 4·2%. The electrocardiogram (ECG) was monitored throughout the experiment. All surgical procedures were performed in conformity with National (JO 87-848) and European legislation (86/609/CEE) on animal experimentation, and following strictly the recommendations of the Physiological Society.

Following a 1 h observation period prior to the use of muscle relaxant, during which stability of the ECG and the absence of pupillary reaction during surgery were taken as indicators that an adequate level of anaesthesia had been reached, nictitating membrane retraction, pupil dilatation and accommodation blockade were induced by ocular instillation of neosynephrine and atropine. The ECG and heart rate were monitored following the initial anaesthesia and throughout the whole experiment. We have set the alarm level of the monitor for signalling changes in the heart rate at a threshold of 10% above or below the baseline level measured initially before surgery. Concentration of the anaesthetic in the perfusion was increased by steps of 10% in cases of spontaneous changes in heart rate or if the heart rate changed by more than 10% while pinching the paw of the animal. We seldom observed

changes in the heart rate using this test suggesting that the anaesthesia was at an appropriate level. This test was performed approximately every 2 h except in the rare cases of long-lasting intracellular recordings. Throughout the experiments, which lasted 36–72 h, the monitored physiological parameters, the waveform of the ECG, the heart rate, the end-tidal CO_2 concentration (3·8–4·2%) and the body temperature (38 °C), were kept stable.

Optical correction was assessed by retinoscopy (skiascopy) for kittens less than 8 weeks of age, and by reflection of direct tapetal illumination on a stimulation screen (114 cm) in older animals. The skull was cemented to metal bars rigidly fixed to the Horsley-Clarke frame, which enhanced recording stability. In the case of intracellular recordings, stability was further improved when needed by bilateral pneumothorax and eventually cysterna drainage. Local anaesthetic (Xylocaine, 1%) was applied to all surgical incisions, and ear bars were coated with a lidocaine (lignocaine) gel. Small holes (2 mm diameter) were made in the skull above each hemisphere to give access to the region of area 17 corresponding to the representation of the area centralis (stereotaxic co-ordinates: L1–L2, P1–P3). A recording chamber was cemented on the cranial bone and filled with agar or high density mineral oil (60 000 centistokes; Serva, Feinbiochemica, Heidelberg, Germany) once the electrode had been positioned above the cortex through a small incision made in the dura.

Recordings

Extracellular single-unit recordings were made with glass micropipettes (impedance ranging between 2 and 20 MΩ) filled with 3 M KCl or potassium acetate, containing Pontamine Sky Blue. The choice of this electrolyte was made in order to control cellular excitability using very small iontophoresis currents. The shape of the action potential was continuously monitored in order to ensure that the same cell was recorded throughout the experiment (for details see Frégnac, Shulz, Thorpe & Bienenstock, 1992). Geniculate fibres were occasionally recorded extracellularly during cortical penetrations. They were identified as such on the basis of their monocular activation, the absence of orientation selectivity, the presence of full-field responses and their ability to follow stimulation at high temporal frequency (> 10 Hz). The laminar position of extracellular cortical recordings was assessed by ejection of Pontamine Sky Blue. At the end of recording sessions, animals were killed by an intravenous overdose of pentobarbitone and perfused via the heart with Ringer solution (0·9% NaCl) followed by 10% (v/v) formol in Ringer solution. Cortical sections were stained with Cresyl Violet and examined for verification of the electrode placement, and for localization of the sites of extracellular injection of dye.

Intracellular recordings were made using 60–80 MΩ glass micropipettes filled with 2 M potassium methyl sulphate (KMS), 3 M potassium acetate (KAc) or 3 M KCl. Impalement was usually achieved by concomitantly ringing the variable buzzer capacitor of the Axoclamp-2A (Axon Instruments), and advancing the electrode tip by a step of 1–3 μm. A small retaining current (−0·1 to −0·2 nA) was applied during the first few minutes and removed after stabilization of the resting membrane potential. The bridge was systematically balanced using a standard hyperpolarizing test pulse (100 ms, −0·2 to −0·4 nA). Input resistance was first estimated by measuring the asymptotic voltage deflection in response to the test pulse, and was also measured off-line from the slope of the current–voltage (I–V) curves. The value of the resting membrane potential was taken as the difference between the voltage during recording and after exiting from the cell (in the absence of retaining current). Spike amplitude was measured from the firing threshold level to the peak of the action potential, and its duration was measured by the spike width at half-height. Voltage and current signals were low-pass filtered (with a cut-off frequency of 10 kHz) and stored on a video recorder or digital audiotape (DAT). Electrodes for the discontinuous voltage-clamp experiments were specifically designed to reduce their capacitive properties: pulling parameters were adjusted to obtain a shorter shank and the electrode was then coated with Sylgard. Their resistances were kept below 65 MΩ and care was taken to decrease the amount of agar filling in the well to reduce capacitance problems. Voltage-clamp recordings were performed in discontinuous single-electrode mode, at a switching frequency of 3–5 kHz (66% duty cycle) and the current trace was filtered at 1–3 kHz. The amplitude of averaged voltage deviations from the holding potential during visual stimulation was 100 ± 100 μV (A. Baranyi, V. Bringuier & Y. Frégnac, unpublished observations). The quality of the clamp was monitored during the experiment using the monitor signal from the headstage ensuring that the cycle duration was twice as large as the time constant of the electrode. Patch-clamp whole-cell recordings were obtained with low impedance (4–5 MΩ) pipettes containing gluconate solution (mM: 140 potassium gluconate, 10 Hepes, 4 ATP, 2 $MgCl_2$, 0·4 GTP and 0·5 EGTA). In this latter case, voltage clamp was achieved in continuous mode. EEG was monitored using differential recordings from two transcranial screws located above the parietal cortex or close (< 4 mm) to the intracellular recording site. The signal was amplified 20 000 times, bandpass filtered (2–200 Hz), and stored on the DAT recorder.

On- and off-line data processing was done using custom-written software (Acquis1; Gérard Sadoc, CNRS and Biologic, Isère, France) running on an AT 486 computer, and acquisition for the present study was typically made at 4 kHz feeding a 12-bit A/D converter, after low-pass filtering (8-pole Bessel filter) at half of the sampling frequency. This filtering reduced apparent spike amplitude in all cells and especially in fast-spiking cells.

Visual stimulation

Visual responses were assessed first using a hand-held projector. The minimum discharge field (MDF) was then mapped on a drawing table using a back-projector projecting through a 45 deg semitransluscent screen (for details see Frégnac *et al.* 1992). After determining optimal stimulus parameters (orientation, ocularity, velocity and size), the visual activity of the cell was quantitatively studied. The responses to a computer-driven set of stimulus configurations were determined using commercial software (VS, Cambridge Electronic Device) driving an image synthesizer for CRT (controller: Picasso (Innisfree); screen: 608 Tektronix oscilloscope, standard Phosphor 31, luminance range 15–50 cd m^{-2} and contrast 0·4–0·8). The refresh rate used was 100 Hz and one frame was sufficient to draw the stimulus.

During extracellular recording, we studied visual responses to three different sets of parameters: (1) in twenty-one cells, the receptive field (RF) was stimulated monocularly with moving light bars ('dynamic mode') at the optimal and a non-optimal orientation; (2) in twelve cells, a stimulus of a fixed orientation was shown through each eye in alternation; (3) in fifty-eight cells, the spatial organization of the RF was explored in the following way: an optimally oriented bar was shown monocularly (through the dominant eye for non-binocular cells), in the six following configurations: (1–4) back and forth movements for two opposite contrast polarities (bright and dark 'dynamic' bars), (5) and (6) 'on' and 'off' 'static' presentation of the same light bar in at least two positions of the discharge zones of the MDF. In intracellular experiments, twenty-five cells were stimulated with bright bars

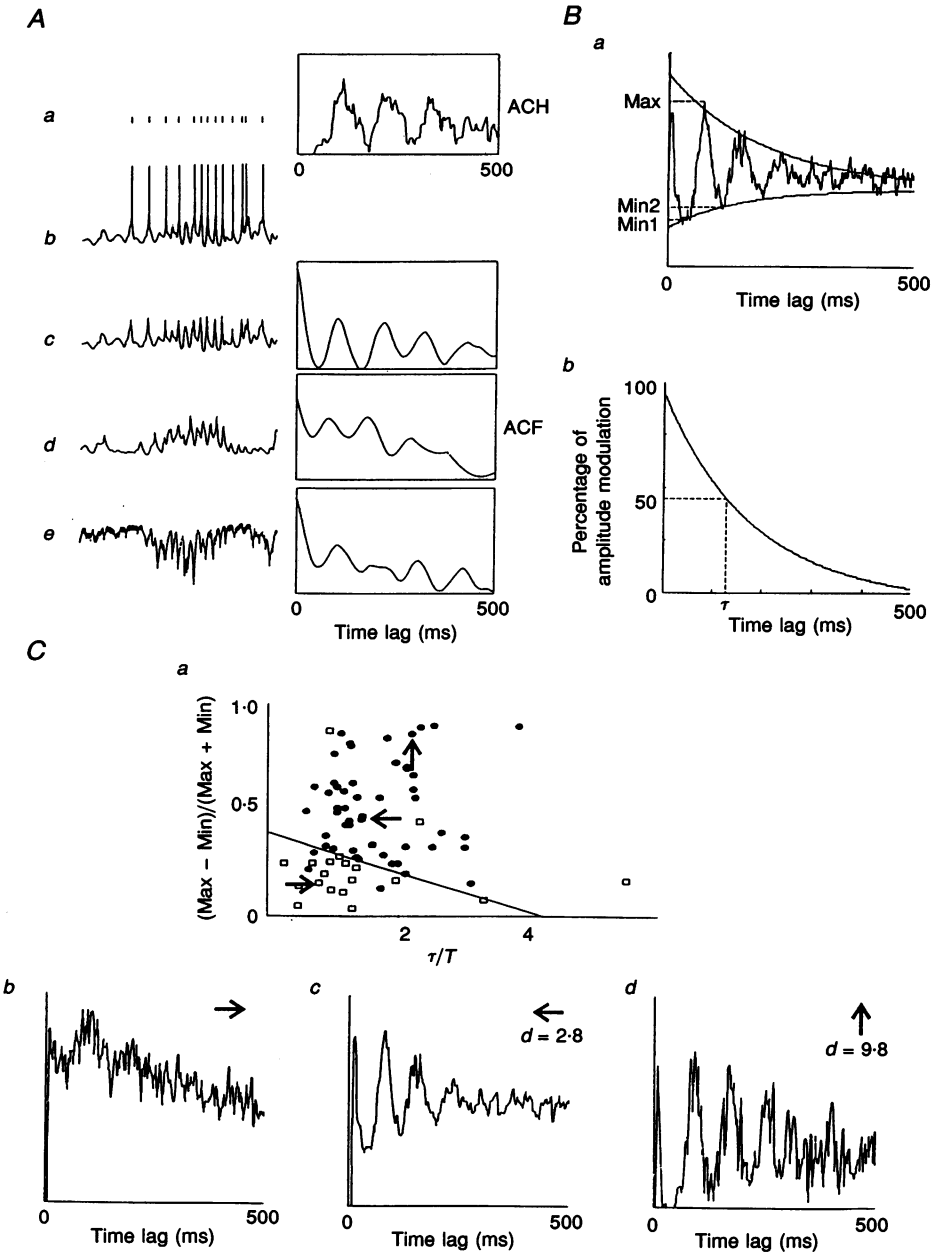

Figure 1. Detection of oscillatory activity

A, raw data and autocorrelation functions. Left column, from top to bottom: *a*, spike train extracted from either intracellular or extracellular recordings; *b*, membrane potential recorded in bridge mode without DC current; *c*, same record as above but after spike filtering; *d*, membrane potential when a negative DC current was injected into the cell; *e*, membrane current when the cell is voltage clamped at its resting potential (inward currents are downward). Right column shows autocorrelation histograms (ACHs) or autocorrelation functions (ACFs) computed for rhythmicity assessment. The ACH computed in the top panel is a cumulative histogram obtained from 10 successive spike trains evoked by the same stimulus. The 3 ACFs shown in the lower panels correspond to individual traces on the left. However, the correlation functions used in this study for rhythmicity assessment were always cumulated over a minimum of 8 trials. *B*, extraction of parameters from ACF and ACH. *Ba*: the first parameter was the 'contrast' of the first side peak (C_m), and defined as the ratio of its maximum ordinate and the mean of its 2 flanking minima; the second parameter was derived from the fitting of the first 3 maxima and the first 4 minima by 2 exponentials that are represented here superimposed on the original ACH. *Bb*: the difference curve between the 2 exponentials gives a time constant (τ) of the damping, defined as the time value for which a 50% decrease was observed. *Ca*, for each ACH or ACF, the 2 parameters, the 'first peak contrast' (C_m) and the damping time constant normalized with respect to the oscillation period (τ/T), were plotted in the C_m–(τ/T) plane; □ represents correlograms that were estimated non-oscillatory by the observer, and ● represents those that were estimated as oscillatory. A linear separation could be obtained by pocket

moving at optimal velocity and for the preferred orientation in both directions. In a few cells, effects of changes in orientation, contrast and velocity were also studied. Thirty-seven cells were stimulated with bars flashed 'on' and 'off', in most cases in two positions of the receptive field.

Data analysis

For the extracellular signal, on-line peristimulus time histograms (PSTHs), time interval histograms (TIHs; i.e. the distribution histograms of all the first-order intervals between the spikes) and autocorrelation histograms (ACHs; i.e. the distribution histograms of the intervals of every order) were computed off-line within a given sequence of stimulation. Histograms were then cumulated over trials. ACHs were usually computed from zero to a maximum time lag of 500 ms (or less for shorter responses), with a 1 or 2 ms binwidth, for eight to twenty iterative presentations of the same stimulus.

The autocorrelations performed on different types of signals are summarized in Fig. 1*A*. ACHs (top right) were computed from spike trains obtained from extracellular or intracellular data (Fig. 1*A a* and *b*). In case of intracellular recordings, in order to obtain a quantitative description of membrane potential oscillations comparable to that of the extracellular signal, the autocorrelation function (ACF) was computed after removing spikes from the membrane potential record. The filtering procedure is based on detection of instantaneous time derivatives in the membrane potential (Fig. 1*A c*). ACFs were also generated from subthreshold membrane potential fluctuations obtained by hyperpolarizing the cell with a negative DC current while the receptive field was visually stimulated (Fig. 1*A d*). Finally, we computed the ACF of membrane currents while the cell was voltage clamped (Fig. 1*A e*).

The presence of oscillations (rhythmicity) in spike trains was revealed by regularly spaced peaks in the ACHs. This cumulative measure excluded transient oscillatory behaviour from the analysis, which could be dominant in one trial but absent in the others, or which changed in frequency across trials. Oscillatory ACHs often showed damped peaks, but the pattern itself varied from one cell to the other. In some instances, the ACH could be fitted by a Gabor function (product of a cosine by a Gaussian function), but it was far from a general rule. Generally, the shape of the peaks did not match that of the Gabor template, because their flanks were too asymmetric. Furthermore, the Gabor approach is devoid of theoretical background. A two-step template-free analysis was therefore applied in order to assess the presence of oscillations. ACHs were tagged as oscillatory if: (a) their peaks were patterned in a rhythmic fashion; and (b) their amplitude was larger than a given threshold. Although the following processing description focuses on ACHs, the same analysis was applied separately to ACFs.

Step (a). In the first step, local extrema were defined as points (x, y) of the ACH that have a maximum or minimum y value within an $(x - l, x + l)$ interval (where l is half the width of the moving window). The interval itself was displaced as a moving window along the time axis from zero to 500 ms. In the case where several local extrema were detected in a given interval, the one with the smallest abscissa value was selected. In order to scan a broad spectrum of temporal frequencies with accuracy, the width of the moving window was progressively varied ($l = 5$, 10, 20, 30, 40, 50, 60, 80 and 100 ms). This scanning was performed on smoothed ACHs (to reduce local variability): a uniform 7 ms smoothing (i.e. each point was substituted by the mean value of its neighbours in a 7 ms window centred on it) was applied to ACHs scanned with l values ranging from 5 to 20 ms, and a uniform 31 ms smoothing was applied to ACHs scanned with l values ranging from 30 to 100 ms. No smoothing was applied to the ACFs.

Activity was judged as rhythmic if the two following criteria were met. (1) Four minima and three maxima (the first one occurring after the first minimum) were sought in the ACHs. If this number of extrema was not reached, the ACH or the ACF was tagged as non-oscillatory. (2) Alternating minima and maxima were considered regularly spaced if the coefficient of variation (ratio of standard deviation over mean) of the interval distribution of the six intervals (three between the minima, two between the maxima and the latency of the first maximum) was less than 0·16. This threshold value was empirically determined by examining a sample of ACHs computed from artificial spike trains. Several pseudo-periodic point processes were generated by adding a Gaussian jitter of null mean (positive or negative) to a fixed time interval, and ACHs were compared for progressively higher and higher variation coefficients of the Gaussian noise. The rhythmicity threshold was set such that three peaks detectable by an observer appeared in the ACH.

The fact that the time excursion of the ACH was limited to a 500 ms lag duration and that at least four minima were required for significant oscillation detection implies that the oscillation spectrum was high-pass filtered at 7 Hz. Because of the extrema definition (see above) and the chosen minimal l value of 5 ms, our maximal frequency resolution was limited to 200 Hz. However, because of the 7 ms uniform smoothing procedure of the ACH, we observed that oscillations above 85 Hz tended to be reduced. The method is therefore characterized by a 7–85 Hz bandpass filtering. Note that this procedure allows the extraction of several frequencies from the same ACH.

Step (b). In the second step, two parameters (Fig. 1*B*) that quantified peak amplitudes were extracted from the ACHs (and ACFs) that had satisfied the previous rhythmicity analysis. The first parameter is C_m, the 'Michelson contrast' of the first peak for extracellular data, i.e.:

$$C_m = (\text{Max} - \text{Min})/(\text{Max} + \text{Min}),$$

where Max is the amplitude of the first peak and Min the averaged amplitude of the first two minima (Min1 and Min2 in Fig. 1*B*). The second parameter is a time constant τ characterizing the damping of the modulation, and is defined as the difference between the two exponential curves (of the type $a_1 \exp(a_2 x) + a_3$) fitting the four maxima and the three minima, respectively. τ was chosen by

algorithm running on a perceptron (see Methods for details). Three representative examples are given in *C b*, *c* and *d*. *C b*, the ACH was estimated as non-oscillatory and its representation in the C_m–(τ/T) plane was situated under the separation line (arrow to the right in *C a*). *C c* and *d*, ACHs were estimated as oscillatory but were distinguished by the Euclidean distance of their associated circle and the separation line ($d = 2{\cdot}8$ and 9·8, respectively), which provided a quantitative *rhythmicity index* for the strength of the oscillation observed in the ACH.

convention as the delay for which the amplitude of the oscillatory component was reduced by half, and was normalized with respect to T, the period of the rhythmicity (as in Engel, König, Gray & Singer, 1990), defined by the average interval between maxima and minima (see above).

Each ACH was then plotted in the C_m–(τ/T) plane and was tagged as oscillatory or non-oscillatory according to the location of its representative point in the plane (Fig. 1*C*). The linear partition of the plane between a rejection zone and a region where oscillatory behaviour is recognized was obtained by feeding a perceptron (pocket algorithm; Gallant, 1986) with point co-ordinates in the C_m–(τ/T) plane and their corresponding classification made by a human observer (required to detect at least 3 peaks). Only six out of the seventy-one experimental ACHs were judged 'oscillatory' by the observer but fell in the rejection zone of the classification plane (or reverse). In twenty-nine other ACHs no damping time constants could be extracted because of the lack of monotonous decrease in peak amplitudes from the first to the third maximum. These non-damped ACHs were therefore classified as oscillatory or non-oscillatory on the sole basis of the C_m parameter, and the empirical threshold found for that separation was 17%. Three out of the twenty-nine non-damped ACHs were classified differently by the algorithm and the observer. Thus, the mismatch between the two classifications concerned only nine out of one-hundred ACHs (91% of agreement).

Following the same method, thirty-eight ACFs from intracellular data were described by two parameters: C_1, that corresponded to the maximal value of the first peak in ACFs normalized to 1; and τ/T, as defined for extracellular data. Linear partition in a separate C_1–(τ/T) plane gave only two category mismatches between the perceptron-based algorithm and the observer classification. Six non-damped ACFs were separated using a C_1 threshold value of 7·5% that gave one mismatch. A total of three mismatches were found out of forty-four ACFs (93% agreement). Note that because no smoothing is applied to ACFs, the filter associated to the algorithm applied to intracellular data has a 7–200 Hz bandpass.

The final classification that was retained was that of the algorithm. Decision based only on the human observer accounts for this classification with an overall accuracy of 91·6%. From the C_m–(τ/T) and C_1–(τ/T) plots, a *rhythmicity index* was defined for each ACH and ACF as the Euclidean distance from its representative point to the separation line determined by the pocket algorithm (see Fig. 1*C*). The performance of our rhythmicity detection method was compared with that used by Ghose & Freeman (1992), which was based on the measure of the signal-to-noise ratio derived from the power spectrum of the ACH. Both analyses were applied to the artificial pseudoperiodic trains described in step (a) and characterized by Gaussian distributions (fixed mean with a variable standard error). The two measurements gave very similar results. However, our method could discard spike trains where spike doublets occurred very frequently and gave rise to a single lateral peak in the ACH, whereas the method of Ghose & Freeman (1992) would tag such data as oscillatory.

To distinguish possible oscillations propagated from the stimulus itself and hence time locked to its onset, 'shuffled' cross-correlograms were computed between the spike trains of two consecutive trials in response to the same stimulus and analysed similarly to the ACHs. Three ACHs and one ACF were discarded from the analysis, because their corresponding shuffled cross-correlograms and cross-correlation function were significantly modulated.

RESULTS

Ninety-two cells were recorded extracellularly and seventy-six intracellularly in area 17 of kittens (4–24 weeks of age) and cats. The duration of intracellular recordings ranged between 10 and 240 min. Cells with a resting membrane potential more negative than −50 mV, a spike amplitude larger than 50 mV (except for fast-spiking cells for which spike height has been reported to be curtailed by a stronger repolarization process), and a spike width at half-height of less than 1·1 ms (measured on an analog large-bandwidth oscilloscope before final digitization) were selected for further analysis ($n = 76$). Means ± S.D. were: −63 ± 7 mV for membrane potential; 63 ± 10 mV for spike amplitude; 0·7 ± 0·2 ms for spike width at half-height; and 25 ± 12 MΩ for input resistance (range, 9–75 MΩ).

General characteristics of oscillating cells

One-third of the cells (55 out of 168) showed significant oscillations during visual activation and to a much lesser extent (5 out of 168) during spontaneous activity periods. For any given set of stimulus configurations, this proportion was the same in the extracellularly and intracellularly recorded populations. Although the frequencies of these oscillations covered a large spectrum (from 7 to 72 Hz), 93% of oscillatory ACHs or ACFs showed significant rhythmicity below 20 Hz, with a predominance in the 7–14 Hz band (Fig. 2*A*). No correlation was found between the strength (see Methods) and the frequency of the oscillation.

We examined the age dependence of oscillatory behaviour. The proportion of oscillating cells was constant across age classes and no correlation was observed between oscillation frequency and age ($r = +0{\cdot}15$, $F = 1{\cdot}66$ and $P > 0{\cdot}2$ for extracellular recordings; and $r = +0{\cdot}11$, $F = 0{\cdot}28$ and $P > 0{\cdot}6$ for intracellular recordings). However, some of the rhythmic cells in the youngest kittens (4–6 weeks old) showed highly rhythmic patterns of discharges that were reflected by a larger oscillatory index (Fig. 2*B*) than that found in older preparations (Student's t test, $P < 0{\cdot}0001$). This pattern was not apparent in the case of intracellular recordings, at least in part because of the small number of cells recorded in kittens less than 5 weeks of age.

Because oscillatory behaviour might result from the pace-maker properties of a specific neuronal population, we looked for possible correlations of oscillatory behaviour with the laminar location, the intrinsic firing mode of the recorded cells and the receptive field type. (1) Laminar analysis (extracellular recordings) revealed that the set of oscillatory cells could not be distinguished from a random sample of the total population. Neither oscillation strength nor frequency distribution showed any layer bias. (2) Firing modes determined on the basis of intracellular response patterns to current step injections were classified using criteria similar to those defined in previous studies, *in vitro* (McCormick, Connors, Lighthall & Prince, 1985) and *in vivo* (Baranyi, Svente & Woody, 1993): regular spiking (RS),

intrinsically bursting (IB) and fast-spiking (FS) cells. In the second category, neurons were included that displayed a response involving a burst followed by repetitive single spike discharge. Their respective proportions in our sample were 55, 40 and 5%. Intracellular records from oscillatory cells showed mainly bursting behaviour (62·5% of IB, 31% of RS and 6·3% of FS) and the distribution of the different excitability types was significantly different from that of non-oscillatory cells (Fig. 2*C*; χ^2 test, $P < 0{\cdot}01$). The implications of this finding will be further developed in the Discussion. (3) No correlation was found between oscillatory behaviour and receptive field type: simple cells oscillated in a proportion (37%) similar to complex cells (35%).

Extrinsic *vs.* intrinsic origin of oscillations

Three types of neuronal activity are distinguished. 'Background' activity periods correspond to membrane potential fluctuations occurring in the absence of visual stimulation and intracellular current application. Records when the cell was kept hyperpolarized with a constant intracellular DC current are included in the term 'background activity'. 'Current-induced' activity refers to events evoked by intracellular positive current steps (in bridge mode) applied to the cell. Finally, 'visually evoked' activity refers to periods of time where a visual stimulus was flashed or moved in the receptive field of the cell.

Oscillations in background activity

Extracellularly recorded spontaneous spike trains were never found to contain significant rhythmicity when assessed over a time period comparable to that used to study the visual response. However, five out of seventy-six cells recorded intracellularly showed stable spontaneous oscillations (between 7 and 13 Hz), both in terms of subthreshold and spiking behaviour. These cells were identified as RS ($n = 2$), IB ($n = 2$) or FS ($n = 1$) types. Two of these (one RS and one IB) were the only ones out of seventy-two cells recorded with electrodes containing KMS or KAc which showed spontaneous oscillations, and are illustrated in Fig. 3*A*. The remaining cells (one RS, one FS and one IB; see an example in Fig. 3*B*) were recorded with KCl-filled electrodes (3 out of 4 cells studied quantitatively). Qualitative inspection of the intrinsic activity pattern of fifteen other cells (not included in the present sample) out of the nineteen cells which were recorded with KCl confirmed that oscillatory behaviour was greatly facilitated by the filling of the cell by chloride ions. In all cases at resting membrane potential, oscillations consisted of large depolarizing events (5–15 mV) recurring

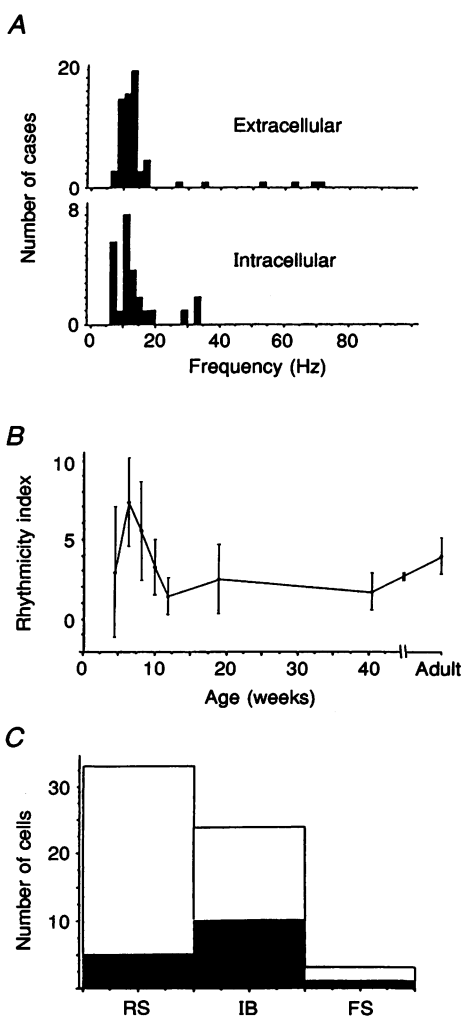

Figure 2. General characteristics of oscillatory activity

A, distribution of frequencies of significant oscillations observed with extracellular (top) and intracellular (bottom) recordings. The bandpass of the algorithm extracting significant oscillatory activity was 7–85 Hz for extracellular data and 7–200 Hz for intracellular data. Note the similarity in the range covered by these 2 frequency distributions. Each case reported corresponds to a neuron stimulated with a given stimulus configuration. *B*, age dependence of oscillatory behaviour. The strength of oscillations (see Fig. 1*C*) was averaged within age categories and plotted as a function of age (weeks; means ± S.D.). Less variability with age and larger mean values were found in 5- and 6-week-old animals (peak of critical period), compared with those 8–10 weeks old. *C*, firing modes distribution. Cortical cells were classified as regular spiking (RS), intrinsically bursting (IB), or fast spiking (FS) as described in Methods. Filled bars represent cells that exhibited significant oscillatory activity; open bars represent non-oscillatory cells. Although RS cells were the most frequent in the global sample, the majority of oscillatory neurons were of the IB type.

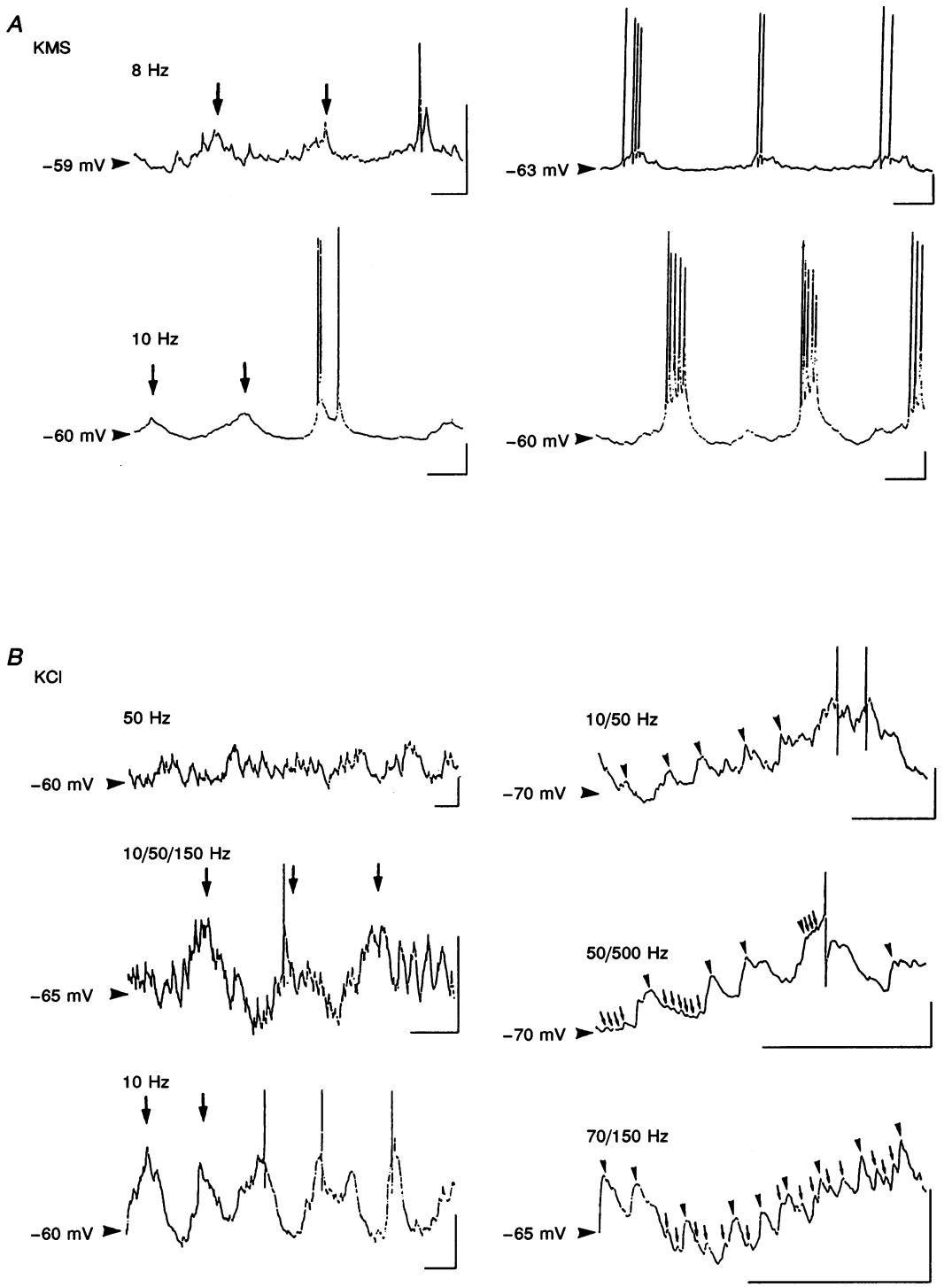

Figure 3. 'Spontaneous' oscillatory activity in cells recorded intracellularly with KMS-filled electrodes (*A*) and KCl-filled electrodes (*B*)

A, the top row shows the oscillatory activity of the same RS neuron in the subthreshold (left) as well as in the spiking (right) domain. Same convention in the lower row, illustrating the case of an IB cell. Periodic subthreshold potentials are tagged by downwards arrows. These cells were the only 2 cases where we recorded stable spontaneous oscillatory activity in KMS recordings (out of 72). Scale bars, 50 ms and 10 mV. Resting potentials are indicated by horizontal arrowheads on the left of the traces, here and in subsequent figures. *B*, episodic oscillations, covering a wide range of frequencies (10–500 Hz) were observed in most cells during recordings with KCl-filled electrodes. Only 2 cells are illustrated here, with the 3 episodes of oscillatory activity in each column corresponding to the same cell. Frequencies above 20 Hz were unstable and not apparent in cumulative ACFs. Periodic subthreshold synaptic potentials are designated by arrowheads (larger size, lower frequency) and small arrows (smaller size, higher frequency). Scale bars, 50 ms and 10 mV.

about every 100 ms. The spiking activity tended to be more intense with KCl electrodes and always occurred riding on the top of subthreshold modulation of the cell membrane potential. KCl recordings could also reveal a true repertoire of rhythmic abilities, during episodes too short in duration (< 500 ms) to reach the significance criteria. Such episodes contained small events (peak amplitude of the order of 1 mV) repeated at frequencies up to several hundred hertz (Fig. 3*B*).

Current-induced oscillations

Intracellular current pulses were applied to characterize the firing mode of the cell, and test its ability to generate rhythmic discharge. RS cells with strong adaptation showed no oscillatory behaviour during current injection. However, some of the RS cells which showed a reduced level of adaptation of discharge after the first two spikes (see also Baranyi *et al.* 1993), and the majority of bursting cells and the fast-spiking cells could exhibit rhythmicity. Some IB cells exhibited an initial burst following the current step onset followed by periodic firing of single spikes, a discharge pattern that has been reported *in vitro* (McCormick *et al.* 1985). As classically described, the evoked frequency increased with the amount of current injected intracellularly. Firing rates up to 60 Hz could be reached in non-adapting cells for currents less than 1–2 nA (see also Jagadeesh *et al.* 1992).

In the subthreshold domain, no consistent oscillatory behaviour was found, although episodic rhythmic fluctuations of membrane potential were observed in two FS cells. Positive subthreshold currents induced an oscillatory response consisting of events of 2–3 mV at 80 Hz, and suprathreshold currents evoked clusters of regularly spaced spikes at a rate of 100–120 Hz. In contrast, the responses elicited by visual stimulation in the same cells showed no oscillations, as revealed by the cumulative ACH.

In summary, two types of rhythmic behaviour were observed in response to current pulses. Periodic firing was observed in poorly adapting RS, IB and FS cells. In the subthreshold domain, only some of the FS cells maintained some rhythmicity, at a depolarization level close to firing threshold. However, in those latter cells rhythmicity was not found in the visual response.

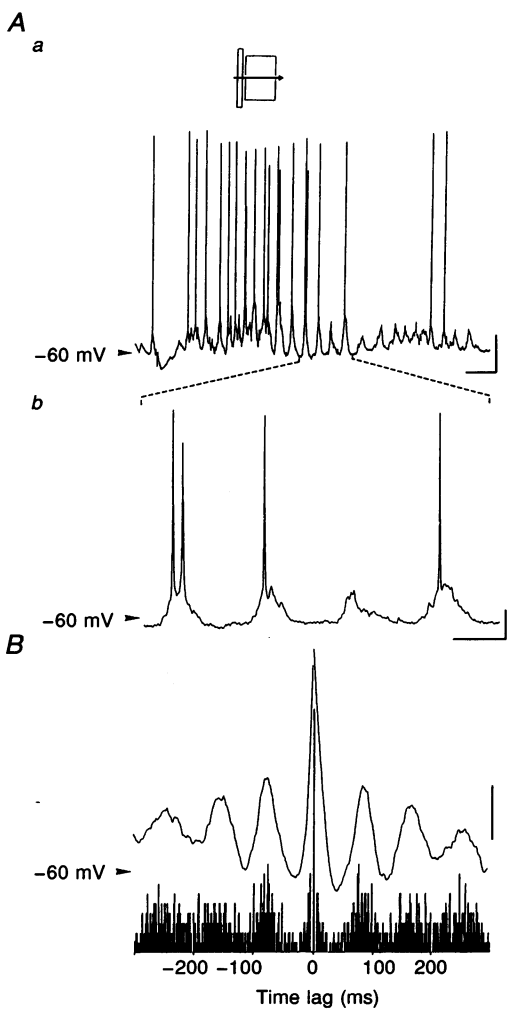

Figure 4. Intracellular visually evoked oscillations in a 9-week-old kitten

A a, response of the neuron to a light bar swept across its receptive field (large rectangle in upper diagram). Some episodes of the oscillatory modulation (narrow rectangle and arrow) remain subthreshold; scale bars, 10 mV and 200 ms. *A b*, expansion from the top trace, showing 4 successive depolarizing events on a faster time scale. Note that some events are separated by a 'dead time' where the membrane potential remains stable, and that the periodicity remains unaltered when the oscillation is subthreshold; scale bars, 10 mV and 100ms. *B*, spike-triggered averaging of the membrane potential cumulated over 10 such trials (continuous line) superimposed on the ACH computed from the discharge in the same trials. Note the similarity in frequency and damping; scale bars, 2 mV and 6 action potentials.

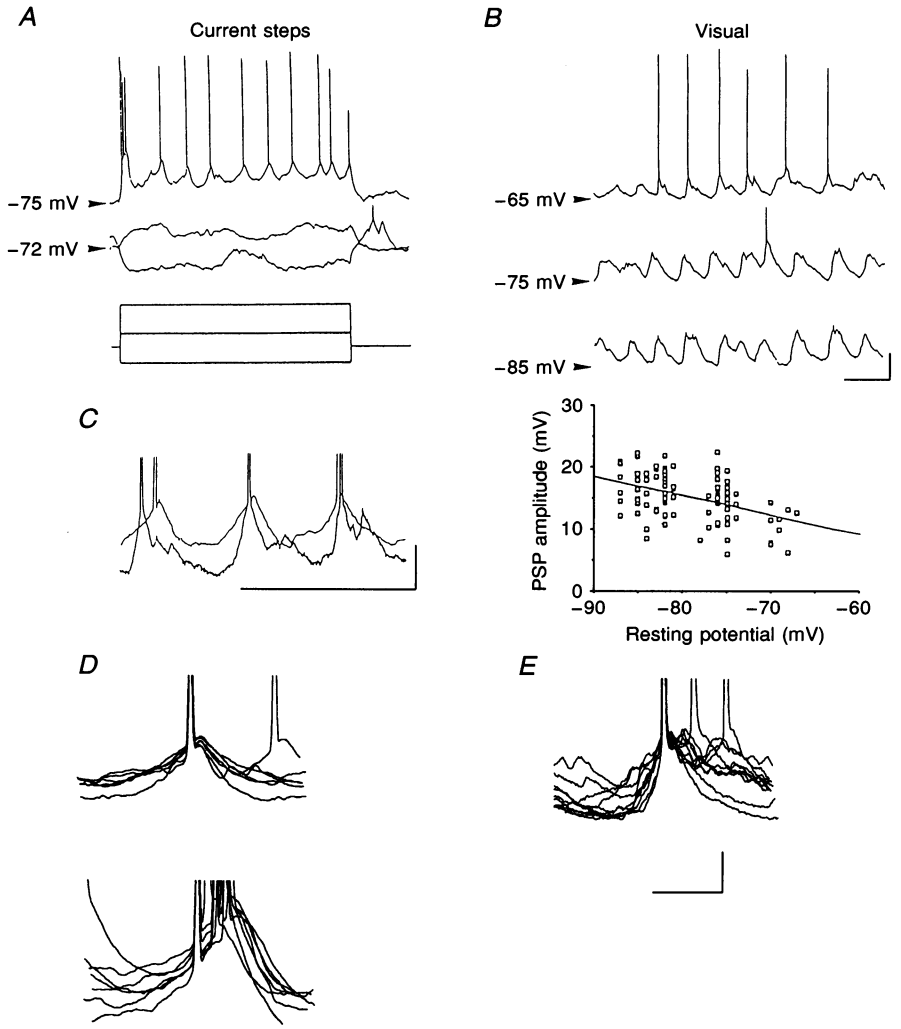

Figure 5. Extrinsic origin of oscillatory behaviour of a complex IB cell, recorded intracellularly in a 9-week-old kitten

A, responses to current pulses (from top to bottom, +2·5, +0·7 and −1 nA). Injection of current pulses alone could evoke rhythmic patterns. However, in contrast to that observed in the presence of visual stimulation, these oscillations were always suprathreshold, and their frequency depended on the amount of current injected (not shown). *B*, responses to a light bar swept across the receptive field. In the absence of DC current injection through the recording electrode, visual stimulation elicited an oscillatory suprathreshold response at 10 Hz (top trace). When hyperpolarized by 10 mV with a −1 nA DC current, the cell responded with a subthreshold oscillatory pattern at the same frequency as in the absence of current. When further hyperpolarized to −85 mV, the frequency still remained unchanged, and the peak-to-peak amplitude of the rhythmic events increased. This behaviour is depicted more quantitatively in the lower frame, where the amplitude of the events is plotted as a function of membrane potential at the initiation of the trial ($r = 0{\cdot}44$, $P < 0{\cdot}001$). A significant linear fit was obtained, suggesting that a simple change in driving force for the different ions mediating these currents might explain this dependency. *C*, in order to superimpose and compare the 2 types of responses, the amount of current injected was adjusted so that the imposed frequency in the absence of the visual stimulus matched that of the visually evoked oscillations. The visually induced oscillatory activity (lower record) showed asymmetric shapes, with fast depolarization and slower repolarization, whereas current step-induced oscillations showed much more symmetric, if not time-reverted profiles. *D*, periodic potentials were extracted from responses to current steps and superimposed so that spikes were aligned. Two types of waveforms associated with the discharge could be distinguished. Top, the most frequent events were slow depolarizations giving rise to a unique action potential and a slightly faster repolarization. Bottom, occasionally, bursts were observed on the top of which rode 2 or more action potentials. *E*, in contrast, periodic potentials elicited by visual stimulation in the same cell had more indented profiles but could still be distinguished by their faster depolarizations, slower repolarizations and smaller ADP than in response to current steps. Scale bars: *A* and *B*, 20 mV and 100 ms; *C*, 10 mV and 100 ms; *D* and *E*, 10 mV and 20 ms.

Visually induced oscillations

Comparison of intracellular and extracellular recordings. Visual stimulation was by far the most efficient way to trigger oscillations in a consistent manner. This behaviour contrasted with responses to intracellular cathodic current injections (see previous section), where the variability of oscillatory behaviour was too high to reach significance criteria. Extracellular recordings of oscillatory cells were characterized by modulated ACHs. Their TIHs always showed a prominent primary peak at the time lag corresponding to the period of the oscillation and sometimes a secondary peak, suggesting that spiking might stem from subthreshold oscillations that may not lead to spike discharge for every cycle of the wave.

Using intracellular recordings, we could directly show in one-third of the cells the existence of oscillations of the membrane potential during visual stimulation with moving bars. Figure 4 presents intracellular oscillatory responses in a cell recorded in a 9-week-old kitten. Expanding the time scale (Fig. 4*A b*) allowed more careful inspection of events contributing to a single period of the oscillation. In subthreshold events a jagged appearance was suggestive of summated individual EPSPs. Moreover, the depolarizing events were often separated by an apparently silent time zone. Such 'isopotential pauses' suggest that fast depolarization cannot be explained solely by voltage-dependent properties.

Intracellularly and extracellularly recorded oscillations most probably corresponded to the same phenomenon because: (1) they share a similar phenomenology in terms of frequency and stimulus dependency (see next section); (2) ACHs computed on spike discharges during a significantly oscillating episode of membrane potential showed a modulation at the same frequency as that exhibited by the ACF computed on the spike suppressed record; and (3) a strict phase relationship between spiking and the membrane potential could be established by spike-triggered averaging of the membrane potential. For instance, the neuron in Fig. 4 had an oscillatory discharge, as shown by the evenly spaced peaks in the ACH in the lower part of the figure, and the periodic changes in membrane potential were in phase with the suprathreshold periodicity, as shown in the upper record of the bottom part of Fig. 4*B*.

Voltage dependency of oscillatory potentials. A more direct demonstration of an extrinsic origin of the oscillations comes from a quantitative study of the dependency of visually induced oscillations on the resting membrane potential. A typical example of a complex IB cell, recorded in a 9-week-old kitten, is illustrated in Fig. 5. A moving bar of light evoked a 10 Hz oscillatory pattern of membrane potential, leading to rhythmic discharge (Fig. 5*B*). When the cell was hyperpolarized by anodal current injections, the oscillatory behaviour of membrane potential was maintained at the same frequency although the cell no longer reached firing threshold. The peak-to-peak amplitude of the subthreshold depolarizing events increased significantly with hyperpolarization, a linear fit giving an extrapolated reversal potential of −32 mV (graph in Fig. 5*B*), that can be accounted for by the composite excitatory and

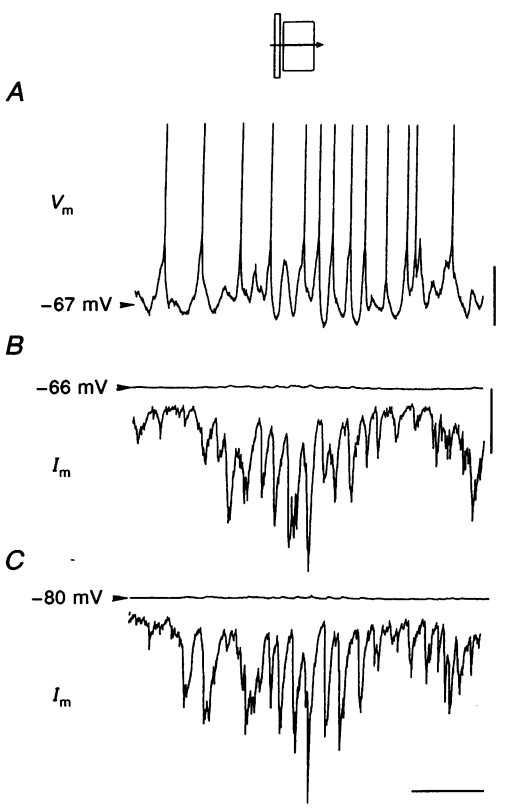

Figure 6. Visually evoked oscillations in voltage and current clamp, in a complex RS cell, recorded in a 9-week-old kitten
Responses of the neuron to a light bar (narrow rectangle and arrow in the diagram) swept across the receptive field (large rectangle). *A*, in bridge mode, starting from a resting potential of −67 mV, a moving light bar evoked a suprathreshold oscillatory response (spikes are truncated) at 9 Hz. *B*, in the same cell, under voltage clamp at −66 mV, visual stimulation elicited large, rhythmic inward currents at 9 Hz. *C*, when held at −80 mV, the cell exhibited inward currents at the same frequency but of increased size with respect to those observed under −67 mV holding potential. Scale bars: *A*, 10 mV (the same scale applies to potentials in the lower traces); *B* and *C*, 200 pA; for all traces, the time scale bar is 500 ms.

inhibitory nature of the compound synaptic potential. This behaviour differed from that observed in the same cell in the absence of visual stimulation, when a current step was applied (Fig. 5*A*). While subthreshold currents evoked no rhythmicity, currents of higher value triggered an oscillatory discharge, the frequency of which depended on the amount of current injected. By adjusting the value of current injected so that the frequency of discharge matched that of the visually induced oscillation, the modulation of the membrane potential in each situation could be directly compared (superimposed traces in Fig. 5*C*). Visual oscillations consisted of events with a depolarization phase faster than that seen during repolarization, while a more symmetric, if not opposite pattern, was characteristic of the current step-induced oscillations. In Fig. 5*D* and *E*, we superimposed several periodic potentials elicited by current and visual stimulation, respectively. Periodic potentials elicited by current (Fig. 5*D*) were categorized in two groups (top and bottom), according to the absence or the presence of a burst. Periodic potentials with single spikes had waveforms showing little variability, with slow depolarization and faster repolarization, while bursts showed faster depolarization but still an asymmetry in the same direction. However, visually evoked periodic potentials (Fig. 5*E*) showed depolarizations faster than repolarizations and jagged profiles. This difference in behaviour suggests that visual oscillations resulted from synaptic events that had a dominant excitatory nature while current injection evoked successions of voltage-dependent phenomena. Furthermore, while current-evoked potentials evoked clear after-depolarizing potentials (ADP) immediately following the action potentials (spatially prominent in the bursting episodes), such components were not as pronounced in the visually induced periodic potentials. When more than one spike occurred within the same current-evoked periodic potential, the intervals between spikes were shorter than those observed during visually elicited bursts.

The dependency of the size of the subthreshold depolarizing events on the membrane potential was assessed in eight oscillatory neurons, including the one presented in Fig. 5. In seven of these cells, their size increased with hyperpolarization from resting potential. The extrapolated reversal potential ranged between −32 and −5 mV. In one

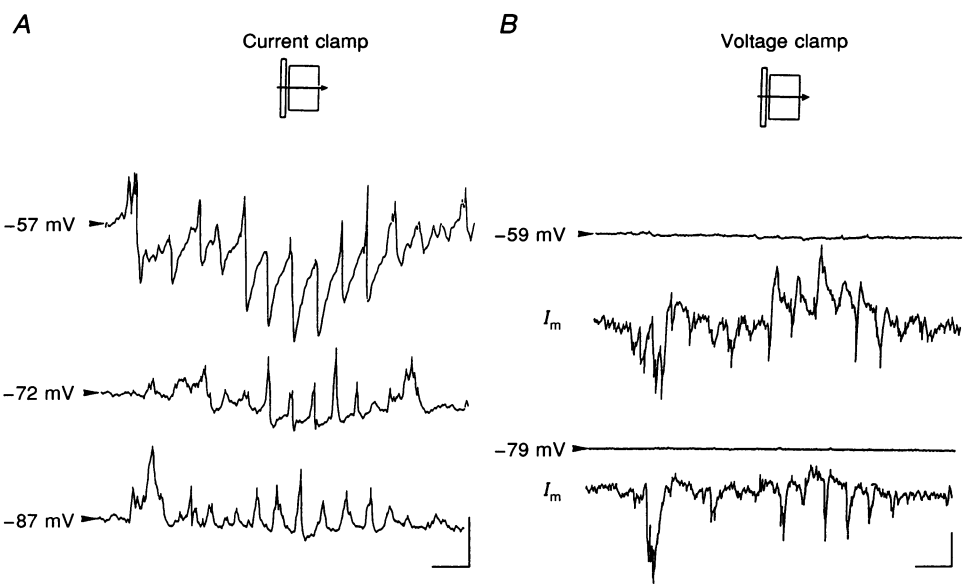

Figure 7. Mixed periodic depolarizing and hyperpolarizing potentials within oscillatory episodes
This neuron was recorded in an 8-week-old kitten and stimulated through the non-preferred eye with a moving light bar (narrow rectangles and arrows in the upper diagrams) swept across its receptive field (large rectangles), and recorded both in bridge mode (*A*) and in voltage-clamp mode (*B*). *A*, at rest (−72 mV, middle trace), the response profile consisted in rhythmic waves of depolarization often followed by a brief hyperpolarization. When the cell was depolarized with a positive DC current (−57 mV, +0·2 nA, top trace), the response consisted of a series of hyperpolarizing events, that could be clearly separated, with sharp onsets and slower repolarizations; in some instances, a small fast depolarization was observed at the end of the cycle, and was abruptly cut by the occurrence of the next hyperpolarizing event. At −87 mV(−0·5 nA, lower trace), excitatory events became larger and longer than at rest, while hyperpolarizing potentials almost disappeared. However, the frequency of the oscillation remained unchanged. Scale bars, 4 mV and 200 ms. *B*, voltage clamped at −59 mV (top), the response was composed of inward and outward currents recurring periodically at the same frequency as that observed in bridge mode. When clamped at −79 mV (bottom), the inward events were larger and longer than at the resting holding potential and the outward currents were strongly reduced. Current traces appear more phasic than voltage records. Scale bar, 50 pA and 200 ms; same scale for voltage traces as in *A*.

cell, we found that anodal hyperpolarization led to a decrease in the size of the depolarizing events. However, very clear subthreshold oscillation persisted (data not shown). The larger amplitude modulation observed at the resting membrane potential might be explained by the involvement of NMDA receptor-mediated transmission or by the presence of voltage-gated currents activated by the depolarizing synaptic responses. However, the rhythm itself seemed to be determined by periodic synaptic input since hyperpolarization did not evoke significant changes in the frequency of oscillations. In contrast, cells could behave rhythmically under current injection and at the same time show no periodicity in visual firing.

Voltage-clamp evidence for rhythmic synaptic currents. If oscillations mainly stem from periodic synaptic inputs, a straightforward prediction is that one should be able to observe them in voltage-clamp recording mode. Four neurons that showed significant visually elicited oscillatory behaviour in bridge mode were studied under single-electrode discontinuous voltage clamp, during which rhythmic inward currents at a similar frequency were evoked. The case of a cell recorded in a 9-week-old kitten, stimulated with a moving bar, first in current clamp, then in voltage-clamp mode, is illustrated in Fig. 6. In current clamp, while the resting potential was fluctuating around −67 mV, visual stimulation induced periodic depolarizations often leading to spikes, at a dominant frequency of 9 Hz (Fig. 6*A*). The same stimulus presented while the cell was voltage clamped at −66 mV triggered a succession of inward events of 200–400 pA, appearing in a rhythmic fashion at the same temporal frequency (Fig. 6*B*). When the cell was clamped at −80 mV (Fig. 6*C*), the frequency did not change ($P > 0{\cdot}4$, t test) but the size of the events increased significantly ($P < 0{\cdot}001$, t test). Linear extrapolation gave a reversal potential of +4 mV, which might indicate that inhibition was completely absent from this response. The inward current values found in this cell were among the largest of those found in oscillatory neurons recorded in voltage clamp using sharp electrodes ($n = 7$). Indeed, amplitudes of 100–200 pA were more common.

The current response of the neuron in Fig. 6*B* and *C* exhibited a slow inward envelope that might be in part expected if the duration of single inward events composing each period is longer than the period itself. However, in some cells the duration of these events was much shorter than the period, so that they were separated by an apparent silent period where no change in transmembrane current was observed (see Fig. 4*A b* for example). These 'pauses' already noticed in current clamp had a mean duration of 35% of the period, when recorded in voltage-clamp mode. This pleads once again in favour of separated synaptic events rather than a regenerative process involving voltage-dependent properties.

Involvement of inhibitory inputs. The focus of our analysis has so far been centred on synaptic input of excitatory nature. However, in three cells we were able to record visually evoked rhythmicity where each period of the oscillation contained an apparent alternation of excitatory–inhibitory events. In one of these cells, while the response to the dominant eye consisted of a rhythmic sequence of

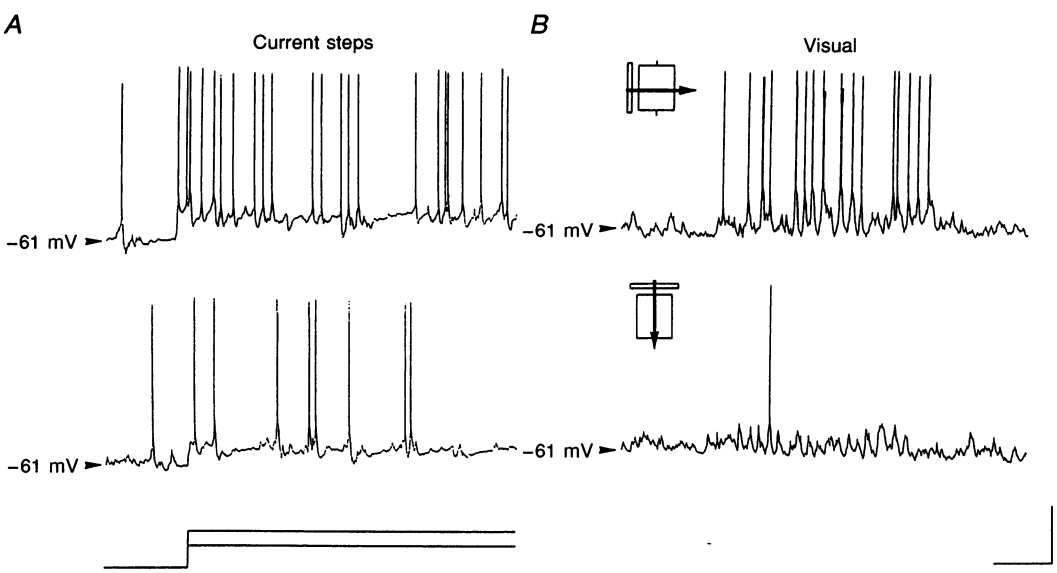

Figure 8. Visually evoked oscillations in the γ range frequency band

A, this complex IB cell recorded in an 8-week-old kitten was stimulated by +0·5 nA (top) and +0·3 nA (bottom trace) current steps in the absence of visual stimulus. No significant oscillatory pattern could be elicited. *B*, sweeping a light bar (narrow rectangles and arrows) across the receptive field (large rectangles), both at the preferred (top trace) and orthogonal (bottom trace) orientations evoked oscillatory responses at 33 Hz at the supra- or subthreshold level, respectively. Scale bars, 200 ms and 25 mV.

depolarizing and spiking events (data not shown), stimulation through the non-preferred eye evoked a response of alternated depolarizing and hyperpolarizing events (shown in Fig. 7). The resting potential of this cell was −72 mV. When depolarized to −57 mV, the visual response in bridge mode was marked by periodic hyperpolarizing events of 2–4 mV, separated in some cases by fast depolarizations (Fig. 7*A*, top trace). These excitatory potentials were cut by the inhibitory ones. Repolarizing to −72 mV and further hyperpolarizing the membrane to −87 mV with a negative DC current led to an attenuation of the inhibitory events, and an enhancement of the excitatory ones, both in amplitude and duration (Fig. 7*A*, bottom trace). The current-clamp records alone could not determine if this excitatory periodic activity depended on intrinsic properties of the neuron that are interrupted by inhibitory synaptic input at more depolarized membrane potential levels, or if both the excitatory and inhibitory events stemmed from synaptic activation. The voltage-clamp recording performed on the same cell for identical stimulus conditions, as shown in Fig. 7*B* showed alternance of inward and outward currents when the cell was clamped at −59 mV, whereas inward currents were dominant when the cell was clamped at −79 mV, therefore indicating that these events were of synaptic origin.

Under all these recording conditions, the ACFs for this cell remained oscillatory at the same frequency, thus demonstrating independence in the frequency domain between the inward and outward components at the post-synaptic level. The time lag between the inward and outward currents corresponded to a 45 deg phase shift between excitation and inhibition during the oscillatory cycle. This phase shift did not depend on the direction of the bar moving along the axis orthogonal to the preferred orientation and therefore could not be explained in terms of the spatial organization of the receptive field. Since, in the same cell, the response to the dominant eye contained suprathreshold oscillations (data not shown) devoid of apparent hyperpolarizing events, these results also show that the imbalance in the level of inhibition elicited from each eye might contribute to the ocular dominance of single cortical neurons.

γ range oscillations

The oscillations in neural activity we have discussed so far concern the α and β frequency ranges. Very seldomly did we record oscillations above 20 Hz. Two cells recorded intracellularly exhibited oscillatory frequencies above 30 Hz (32 and 33 Hz) when stimulated with a moving light bar. The complex IB cell shown in Fig. 8 was stimulated both with drifting light bars and positive current steps. Visual stimulation at optimal orientation evoked a powerful oscillatory pattern at 33 Hz. Each period of the oscillation was marked by a burst-like depolarization, triggering one to five action potentials. When stimulated at orthogonal orientation, a clear subthreshold oscillatory response was

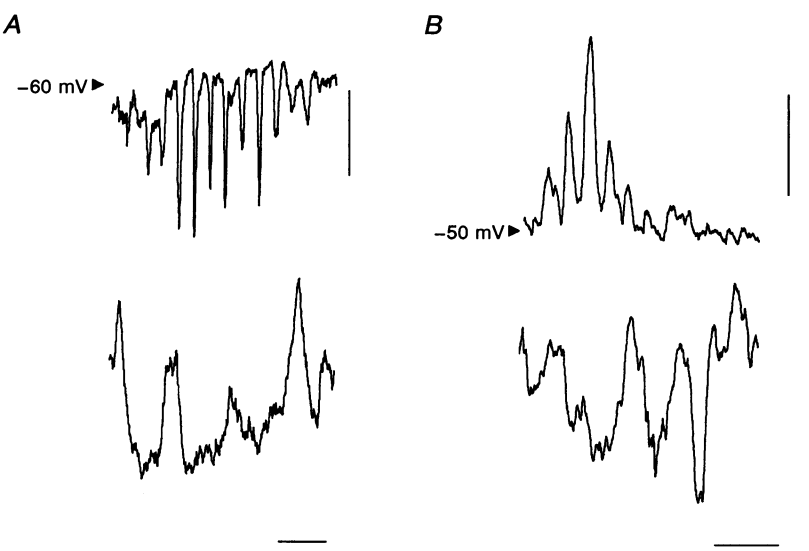

Figure 9. Absence of correlation between intracellular oscillations and local EEG

A, this simple cell was recorded in whole-cell, continuous voltage-clamp mode with QX314 in the pipette, in a 12-week-old kitten. Top: I_m, during stimulation by a bar swept across the receptive field at optimal orientation and speed. Bottom: simultaneously recorded EEG, less than 2 mm from the penetration site. Oscillatory inward currents (14 Hz) were evoked by visual stimulation whereas the EEG showed no rhythmically organized pattern. Scale bars, 0·4 nA (top trace) and 200 ms. *B*, a second simple cell recorded in bridge mode in a 12-week-old kitten with a sharp electrode containing QX314. Top: V_m, during a stimulation by a bar swept across the receptive field at optimal orientation and speed. Bottom: EEG recorded simultaneously, less than 2 mm from the penetration site. Oscillatory depolarizations (31 Hz) were evoked by visual stimulation, whereas the EEG showed no rhythmically organized pattern. Scale bars, 10 mV (top trace) and 100 ms.

evoked at the same frequency. However, current step injections alone did not evoke any stable oscillatory discharge, nor subthreshold rhythmicity. The intraburst frequency observed during optimal visual stimulation could reach 500 Hz, which is a much higher value than that typically observed during slower oscillatory activity (up to 200 Hz).

Absence of correlation of unitary responses with EEG

As stated earlier, most oscillatory responses we observed were in the 8–20 Hz range, which raises the issue of their dependency on the state of anaesthesia of the preparation, and more specifically of their relationship with sleep spindles. In fact, it could be argued that under our conditions of anaesthesia, visual stimulation might activate the thalamic mechanisms generating spindles, that could propagate to the visual cortex. This would be in agreement with the synaptic origin of the cortical rhythms we recorded. We therefore examined the EEG recorded at the primary visual cortex level. A first observation is that in our preparation, during anaesthesia with Althesin, a synthetic steroid, EEG spectrum peaks were typically restricted to the 4–7 Hz range, a lower frequency than that of the visually evoked oscillations. A second argument comes from the direct comparison of single neuron behaviour and surface EEG recorded simultaneously at close distance (< 2 mm from the penetration site). Seven intracellular recordings were performed in these conditions. In no case did we observe spindles or higher frequency oscillations (> 7 Hz) in the EEG during the visual stimulation. However, two cells showed oscillatory behaviour and are illustrated in Fig. 9. One cell was recorded in voltage clamp (whole-cell mode, Fig. 9*A*) and the other intracellularly, in bridge mode (Fig. 9*B*). Both cells were recorded with 2(triethylamino)-*N*-(2,6-dimethylphenyl)acetamide (QX314) in the pipette, in order to block fast and persistent sodium channels and potassium channels. Although QX314 and, in one of the cases, voltage clamp, are expected to maximize the influence of synaptic activity on the behaviour of the cell, no correlation could be observed between the periodic inward currents (or depolarization) and the concomitantly recorded EEG. Furthermore, when studying long time periods of extracellular recorded activity, oscillations in the background firing rate were mostly transient and never in the same range of frequency as those observed during the visual stimulation. A last argument pleading for a lack of correlation between EEG and cellular activity during visual responses is that different oscillation frequencies could be recorded in the same neuron in response to opposite contrast stimuli during interleaved trials. Therefore, the oscillatory responses we have observed at the single cell level cannot be accounted for in terms of massive synchronization, such as those underlying spindles or α rhythm.

In summary, the oscillations we observed both in the spike trains and membrane potential are generated pre-synaptically from the recorded cell. Because we could not record neurons that behaved as pacemakers during visual stimulation, we conclude that rhythmicity is a result of the network architecture and function, or stems from periodic inputs inherited from afferent activation. Voltage-dependent inherent mechanisms do not contribute to rhythmogenesis of the visually evoked oscillation at the single cell level, although it cannot be excluded that they might determine in a co-operative manner some of the temporal properties of the network.

Stimulus dependency

Visually driven oscillations have been proposed to participate in the neural processing underlying binding and image segmentation and their strength assumed to signal the coherence of the visual input configuration (Fig. 9 in Gray *et al.* 1990). It is therefore of importance to study in a systematic and quantitative way their dependency with respect to the visual stimulation.

General characteristics

Twenty-one of the oscillatory cells recorded extracellularly were all stimulated by light and dark bars, swept at optimal velocity in both directions orthogonal to the preferred orientation, and by stationary stimulus flashed 'on' and 'off' in at least two positions of the receptive field (at least eight configurations of stimulation). Among these, only ten cells oscillated for more than one stimulus configuration. We therefore considered the possibility that some stimuli might be more efficient than others for eliciting an oscillatory response. This was confirmed by the fact that the distribution of occurrence of oscillatory responses with respect to the type of stimulus used was not uniform ($P < 0{\cdot}0007$, t test). As described previously (Tovee & Rolls, 1992), oscillations were more likely to occur when using moving bars rather than stationary ones (15 *vs.* 6 cells). However, the contrast polarity or the 'on' *vs.* 'off' transition polarity (see Methods) did not affect the probability of occurrence of oscillations.

We also attempted to correlate the frequency of the oscillation with the stimulus configuration. We found only three cells where different stimuli evoked statistically significant differences in frequency. In two of these cells, direction or contrast polarity significantly modulated the frequency of the rhythmicity by 20–30% (in the 10–14 Hz range), but the absolute value of the changes remained below 3 Hz. In another cell, a moving bar optimally oriented evoked a superposition of two oscillations at 10 and 70 Hz. If the bar stimulated the receptive field at the orthogonal orientation, only the high frequency oscillation was apparent. However, in all other cases the frequency did not appear to be a coding variable.

Stimulus phase-locked oscillations were found in three extracellularly recorded cells and one intracellularly recorded cell, and were withdrawn from the analysis, as mentioned in the Methods section. They were observed in response to a static stimulus, shown 'on' and 'off' in specific regions of the receptive field, and exhibited frequencies between 10 and 16 Hz. In the intracellular case, the response included a

succession of five to seven depolarizing events showing a damping in amplitude, some being subthreshold. For non-stimulus-locked oscillatory neurons, the phase of the oscillatory component with respect to the onset of the response to a moving bar was highly variable, even for the same neuron and using the same stimulus.

Oscillatory strength and response amplitude

Extracellular population analysis. An extensive study of stimulus dependency of oscillatory behaviour with respect to the response intensity was carried out for the extracellular sample and restricted to the twenty-one oscillatory cells that had been tested with the same set of stimulus configurations (see Methods). The amplitude of responses was computed either by considering the averaged number of spikes per second evoked by a given stimulus (raw response), or by normalizing this value with respect to the maximal response evoked in the same cell by the optimal configuration from the stimulus set (normalized response). Neither the raw (Fig. 10*A a*) nor the normalized response (Fig. 10*A b*) was correlated with the oscillation strength ($r^2 = 0{\cdot}064$, $P > 0{\cdot}19$ and $r^2 = 0{\cdot}013$, $P > 0{\cdot}55$, respectively).

Two other analyses were then undertaken. First, we selected cells that oscillated for only one configuration and computed in each cell the algebraic difference between each normalized non-oscillatory response and the normalized oscillatory response. The distribution pattern of these differences

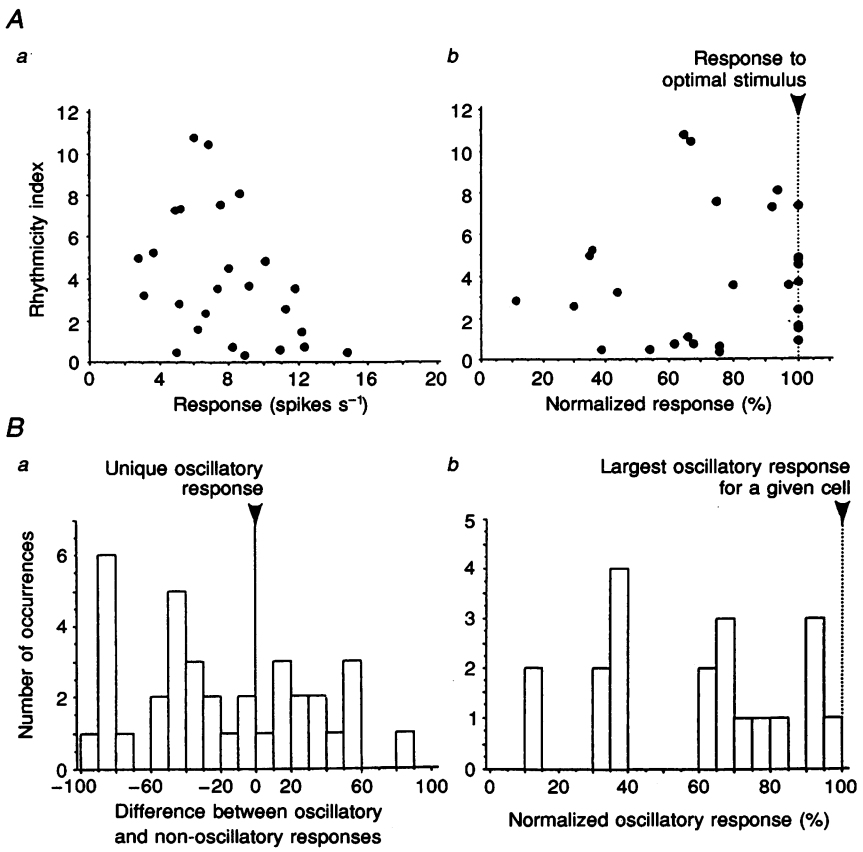

Figure 10. Absence of correlation between response level and oscillatory strength in visual activity

A a, the rhythmicity index (see Methods) of ACHs from a sample of cells, all stimulated with moving and flashed, dark and light bars, is plotted as a function of the raw response amplitude. Three cells having response intensities between 30 and 80 spikes per second are not represented for sake of clarity but are included in the analysis. No correlation was observed between the two parameters ($r^2 = 0{\cdot}064$, $P > 0{\cdot}19$). *A b*, the same data have been plotted again in a plane where raw response intensities for the different stimulus configurations have been normalized with respect to the maximal response intensity obtained in each cell (for a specific stimulus configuration). Still no significant correlation between oscillatory strength and response intensity was observed after this normalization ($r^2 = 0{\cdot}013$, $P > 0{\cdot}55$). *Ba*, for cells which oscillated for only 1 stimulus configuration, it can be seen from the distribution of the differences in normalized response intensity between oscillatory and non-oscillatory responses that, although a trend is observed towards negatives values, non-oscillatory responses could be larger than the oscillatory ones in many cases. *Bb*, for cells of the sample that oscillated significantly for more than 1 stimulus configuration, the distribution of the ratios of the smallest oscillatory response intensity in each cell divided by the largest, indicates that oscillatory responses could be obtained from stimuli giving very different levels of excitation in the same cell.

shows that non-oscillatory responses could be weaker, as strong or stronger than oscillatory responses (Fig. 10*B a*). Thus, in these cells, the oscillatory response was not necessarily the strongest one. Second, for cells oscillating for more than one stimulus, we computed for each cell the ratio of the smallest raw oscillatory response to the largest one. The distribution of this parameter showed that oscillatory behaviour could occur in the same cell for very different response levels (ranging from 10 to 95% of the highest oscillatory response; Fig. 10*B b*). Taken together, these results show that the rhythmicity of the firing does not depend on the strength of visually induced activation.

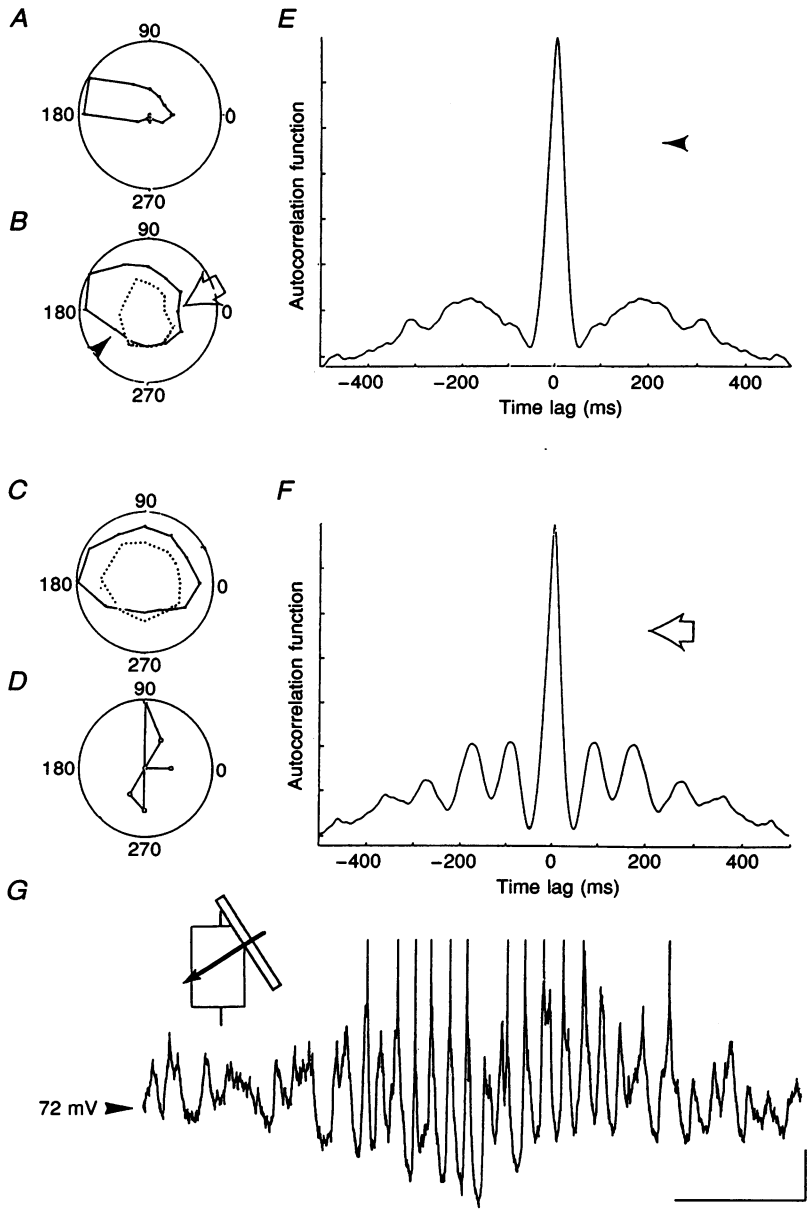

Figure 11. Orientation dependency of oscillatory behaviour in an intracellularly recorded neuron (same cell as in Fig. 5)

The continuous polar curves corresponds to visual activation, and the dotted curves to on-going activity. The 4 tuning curves on the left show the orientation dependency of the various response parameters. Zero degrees corresponds to the reference orientation/direction of the test stimulus shown in *G*, swept across the RF (large rectangle with preferred orientation axis): *A*, number of spikes per trial; *B*, integral of the absolute value of the difference between membrane potential and resting potential after spike filtering; *C*, amplitude of the oscillatory modulation obtained by subtracting the slow non-modulated envelope of the visual response; and *D*, the rhythmicity index as defined in the Methods. *E* and *F* display 2 ACFs cumulated over 10 trials each, and corresponding to responses of similar depolarization amplitude (210 and 0 deg, see *B*). *G* is an oscillatory response obtained using a 0 deg bar (a non-optimal orientation in terms of discharge); scale bars, 400 ms and 10 mV. Membrane potential −72 mV under −1 nA DC current. Spikes are truncated.

Orientation tuning of oscillatory response

It has been suggested that oscillations during sensory activation could help cells to synchronize their activity. Since cross-correlation studies have shown that the strongest synchrony occurs between cells that share similar orientation preference (Ts'o, Gilbert & Wiesel, 1986; Gray *et al.* 1989), one could expect oscillatory behaviour to show maximal strength for the preferred stimulus. In order to test this prediction, we compared orientation tuning of the rate of discharge with that of the oscillatory behaviour of the membrane potential. The complex IB cell shown in Fig. 11 was recorded in a 9-week-old kitten and stimulated with light bars drifting at eight different orientations. Response to a 0 deg (non-optimal) oriented bar is shown at the bottom of the figure. Orientation tunings of four parameters were compared. The top tuning curve (Fig. 11*A*) is a polar plot of the averaged number of spikes in the response represented as a function of the stimulus direction. The cell was directional and orientation selective, and showed a clear preference for 150 deg. The second tuning (Fig. 11*B*) shows the integral of the absolute value of the deviation of the instantaneous membrane potential (after spike filtering) from the mean resting potential computed over the full duration of the visual response. The inner dotted curve represents spontaneous fluctuations of membrane potential integrated for a similar duration. The two tuning curves (Fig. 11*A* and *B*) exhibit similar orientation preference, although the one based on spike counts is more selective than that based on fluctuations of membrane potential (probably due to non-linearity introduced by the spike thresholding). The visual response in this cell could be decomposed into a slow waxing and waning modulation envelope on which rode the oscillatory wave. The third tuning curve (Fig. 11*C*) represents the tuning of the modulation amplitude of the oscillatory response. This modulation is given by the integral value of the spike-suppressed intracellular signal, from which the slow depolarization envelope evoked for each direction of the stimulus has been subtracted, and displays poor orientation selectivity. The bottom curve (Fig. 11*D*) shows the polar plot of the strength of the oscillatory behaviour measured by the *rhythmicity index* (see Methods). This tuning curve indicates that strong sustained oscillations are evoked only for a set of orientations that do not match the tuning of the other parameters. In the present cell, the orientations which elicited the strongest rhythmicity were approximately orthogonal to those evoking the largest discharge intensity. Two examples of ACF are given in Fig. 11*E* and *F*. Although they correspond to a similar amount of subthreshold depolarization (see arrows in Fig. 11*B*), one (open arrow for the 0 deg stimulation; see also Fig. 11*F* and *G*) shows a strong modulation, whereas the other one (filled arrowhead for 210 deg; see also Fig. 11*E*) does not. This orthogonal relationship was not a systematic finding but the absence of correlation between preferred orientations based on spike counts and oscillatory behaviour corroborates the conclusion based on the population analysis presented earlier, in that preferred stimulus parameters in classical terms (in terms of discharge rate) do not allow any predictions about the existence and the strength of rhythmic behaviour.

DISCUSSION

This study is the first comparative analysis of oscillatory behaviour based on similarly large samples of extracellular and intracellular recordings in the primary visual cortex of the cat. A numerical method has been developed to quantify oscillatory behaviour both in spike trains and in membrane potential. This method shows that in both extracellular and intracellular recordings, significant rhythmicity was present in one-third of the recorded cells, mostly during visual activation. The frequencies of the oscillations ranged between 8 and 75 Hz, although 95% were below 20 Hz. Hyperpolarizing currents applied during visual stimulation in current- and voltage-clamp recordings of visual responses allowed us to conclude that periodicity is already present in the synaptic input, and that oscillatory behaviour is likely to be independent of the intrinsic properties of the recorded cells, considered individually. The rhythmic inputs are mainly excitatory, although in a few cells depolarizing events alternated with hyperpolarizing events were observed with a constant phase shift. Using extracellular techniques, we extended our analysis for stimulus features which elicit suprathreshold responses in cortical cells, and this led us to conclude that the strength of oscillatory behaviour is not correlated with the amplitude of the visual response, but rather that these parameters behave independently.

The following discussion is centred on three major issues. (1) How does the occurrence of oscillatory behaviour in our experimental conditions relate to that reported in other published studies? (2) What is the origin of these rhythms? (3) What are their possible functions?

Occurrence and characteristics of visually evoked oscillatory activity

The proportion of oscillatory cells reported in the present study (one-third of the extracellular and intracellular samples) is intermediate between the values observed by Gray *et al.* (1990) (27%), and Ghose & Freeman (1992) (43%), two extensive studies based on extracellularly recorded single units in cat area 17. As initially mentioned by Eckhorn, Bauer, Jordan, Epping & Arndt (1987), this proportion is much lower than values resulting from multi-unit activity and local field potential (LFP) recordings (68 and 75%, respectively; Engel *et al.* 1990). This discrepancy is not limited to the visual cortex. In the olfactory bulb, where it has been shown that spatial patterns of oscillatory EEG activity may carry an informational content, Freeman & Skarda (1985) reported that the powerful 30–90 Hz peaks in the EEG spectrums occurred together with poorly modulated single-unit activity. In the CA1 field of the

rodent hippocampus, Buzsaki, Horvath, Urioste, Hetke & Wise (1992) showed that the field potential oscillations around 200 Hz also occurred together with sparse single pyramidal cell activity, while in-phase cumulating of multiple single-unit responses gave a compound signal highly correlated with the EEG. In contrast, single interneurons of the strata oriens were frequency locked with the EEG.

Since each cell integrates synaptic drive arising from many presynaptic partners, it could be expected that this input sampling might share some similarities with local population recordings such as LFP. For example, in the motor cortex, some EEG events, such as those directly evoked by thalamic stimulation, seizure-related phenomena, barbiturate-induced spindles, as well as some of the spontaneous fluctuations of on-going activity are indeed well correlated with postsynaptic potentials (Creutzfeldt *et al.* 1966). In the visual cortex, our initial hypothesis was that at the cellular level the oscillatory response may be essentially subthreshold, with a probability of occurrence close to that observed using LFP, the demonstration of which required the use of intracellular recording. However, under the present conditions (local stimulation of the receptive field under anaesthesia), it turned out that the occurrence of oscillatory responses was the same in spike trains and subthreshold fluctuations of membrane potential.

Other sources of discrepancy could result from differences in the set of visual stimulation parameters routinely used to assess RF properties. Indeed, since we showed that oscillatory behaviour did not correlate with the largest evoked responses, one cannot exclude that the number of oscillating cells may be underestimated in studies where only a restricted stimulus set of optimal configurations was tested. A last source of variability between studies might result from different statistical tools used to assess the presence of oscillations. This issue has been discussed in details elsewhere (Frégnac, 1991; Young, Tanaka & Yamane, 1992).

The type of neural signal used for the analysis might affect not only the probability of occurrence of oscillatory behaviour, but also the frequency. Namely, single neurons might fire rhythmically at 10 Hz while summated 'population' activity would oscillate at 40 Hz (see for example Kopell & Le Masson, 1994). Indeed, our own study, like others, at the single-unit level, has shown oscillatory behaviour bound in a relatively low frequency spectrum (Schillen, König, Engel & Singer, 1992; Young *et al.* 1992). However, the possibility of frequency multiplexing in our preparation remains unlikely, for two reasons. First, higher frequencies in the activity of single neurons were routinely observed in several studies (Eckhorn *et al.* 1988; Gray *et al.* 1990; Ghose & Freeman, 1992), and were present in our simultaneous geniculate recordings (data not shown). Second, a prediction of the multiplexing hypothesis is that intracellular recordings should reveal the population frequency that was lost in the spike discharge (Kopell & Le Masson, 1994). However, we showed that the same range of frequencies were observed using intracellular and single-unit extracellular recordings (although the distribution of frequencies observed during intracellular recordings shows a second peak – albeit of modest size – in the 30 Hz band, that could be accounted for by the emergence of a harmonic of the dominant frequency; see Fig. 2*A*).

Prominence of the 10 Hz band suggests a possible correlation with EEG waves. Several points argue against this possibility. (1) Oscillatory activity was observed primarily in visually evoked activity and only very rarely in spontaneous activity. (2) The occurrence of oscillatory responses showed a complex stimulus dependency which is incompatible with a non-specific state resonance frequency. Furthermore, in a given cell, the frequency could depend on specific features of the stimulus not necessarily associated with a maximal discharge. (3) Strength of oscillations did not correlate with laminar position, whereas one would expect enhanced periodic activity in layer IV and VI if it was solely derived from thalamic inputs. (4) Visually evoked oscillations were not temporally correlated with surface EEG. This is in contrast to what is observed during barbiturate spindles, where a strong correlation between cellular behaviour and surface EEG is observed (Creutzfeldt *et al.* 1966). In our case, EEG generally displayed lower frequencies, mainly in the 4–7 Hz range, although spindles also occurred. Therefore, even though the steroid anaesthetic Althesin that we have been using might generate spindles in a way comparable to barbiturates, and restrict the range of oscillation frequencies to the lower part of the spectrum, the visually evoked oscillations we observed depended primarily on periodic sources of activation which were not the consequence of global EEG synchronizing states.

The mechanisms underlying the developmental aspect of oscillatory behaviour are largely unknown, but it has been speculated that temporal patterning of neural activity might have a constructive role in the elaboration of cortical networks as soon as propagated activity arises in retinofugal pathways. Our study has shown that oscillatory behaviour in cat area 17 is present from 4 weeks of age, and the strongest oscillatory behaviour was found in cells recorded in 5- and 6-week-old kittens. This latter observation corroborates an earlier observation by Frégnac (1982), that stimulus-locked oscillatory activity and cortical synchronization were most easily produced by periodic full-field stimulation in cortical cells recorded in kitten at the peak of the critical period (4–6 weeks). Moreover, a superposition of 10 and 40 Hz oscillations in the visual responses recorded in area 17 of 4- to 5-week-old kittens has been reported, using precisely the same type of anaesthesia and recording electrodes with which the 40 Hz rhythm is better observed in the adult preparation (Schillen *et al.* 1992). In both frequency ranges, stimulus-dependent synchronization was observed. Although earlier studies from the same laboratory did not report the presence of low frequency oscillations in adult cortical cells,

it cannot be excluded that these were undetected because of the 24–96 Hz filtering procedures applied before oscillation detection (Gray *et al.* 1990). This also applies to the developmental study by Ghose & Freeman (1992) where the peak of detected frequencies is found in the lower range of the analysed spectrum.

Origin of the oscillations

Oscillatory activity was very rare in the background activity. However, when the cells were recorded with KCl, a variety of transient oscillatory episodes were revealed. It is well established that the equilibrium potential of chloride ions shifts during the first minutes of KCl recordings, due to a dialysis of the intracellular medium by the electrolyte of the electrode, and stabilizes around −30 mV (Shulz, Bringuier & Frégnac, 1993). This abnormal frequency of depolarizing events most probably corresponds to a continuous GABAergic bombardment which is not revealed when recording with KMS or KAc, since, in this case, the resting membrane potential is very close to the normal equilibrium potential of chloride ions (−75 mV).

During visual activation, does each recorded cell generate a rhythm when stimulated by a non-modulated input (intrinsic origin), or is the rhythmicity already contained in the afferent activity (extrinsic origin)? Three main reasons support an extrinsic origin. First, in our *in vivo* preparation, we were unable to record consistent subthreshold oscillations triggered non-synaptically. This differs from the subthreshold pacemaker abilities which have been extensively described in some rodent cortical neurons (Alonso & Klink, 1993), but have yet to be reported in the visual cortex of the cat. Second, certain conditions of visual stimulation could evoke subthreshold oscillatory activity, in the same frequency range as the suprathreshold ones. Neither the occurrence nor the frequency of visually evoked oscillatory activity was affected while the cell was hyperpolarized to −80 mV with a negative DC current. At this potential, most conductances (such as persistent sodium, low threshold calcium, and potassium channels) that could be involved in cortical pacemaking are inactivated or de-activated. Third, since one could always argue that a certain set of conductances could generate the rhythm in such a way that the frequency would be independent of the resting potential, we therefore used voltage clamp to 'freeze' voltage-dependent mechanisms during visual stimulation. In these conditions, cells that showed oscillatory behaviour in bridge mode were found to display rhythmic currents during visual stimulation, at the same frequency. In spite of the possibility that, even clamped, voltage-dependent non-inactivated conductances might participate in the genesis of some currents in the conditions of steady-state activation (for example, synaptically mediated calcium influx might trigger outward potassium currents; see Fig. 6 in Markram & Sakmann, 1994), it seems unlikely that they might be involved in the genesis of a repetitive process. Moreover, the fact that oscillatory currents are still present even if the membrane is clamped at a hyperpolarized level rules out any possible contribution of voltage-dependent mechanisms near the electrode impalement site.

Recently, Gray & McCormick (1996) suggested that the intrinsic properties of a newly described category of cells, the 'chattering' cells, could be involved in the generation of γ range visually evoked oscillations. However, the comparison of the oscillations evoked by a visual stimulus and by a positive current injected through the electrode is not as straightforward as it seems. Indeed, the frequencies evoked by current injections and visual stimulation do not always overlap (see Fig. 3 in Gray & McCormick, 1996). Even when the frequencies do overlap, this is not sufficient to ensure that both phenomena share the same (voltage dependent) mechanism. A crucial test would be to replicate the type of experiments done in our study, i.e. to polarize the cell during visual response and see how this affects the frequency and the occurrence of the visually evoked oscillation, and the trajectory of the membrane potential in the two cases (see Fig. 5*D* and *E*).

However, one cannot exclude that voltage-dependent conductances located in the distal dendrites, and thus inaccessible to voltage control, both in bridge mode and voltage clamp, might generate subthreshold oscillations. Several recent studies have shown the presence of voltage-gated calcium and sodium conductances in the dendrites of layer V neurons (Markram & Sakmann, 1994; Stuart & Sakmann, 1994). One observation of special relevance to our study was made by the former group, who showed that single subthreshold EPSPs could trigger calcium transients independently of the activation of NMDA receptors. One might imagine a putative pacemaker system relying on such subthreshold calcium currents and potassium rectifiers under the influence of a tonic synaptic input. However, if these currents were too far away to be clamped, it is difficult to see how their amplitudes could be affected by the DC current that we used to assess their voltage dependency. A putative model of oscillations generated at the dendritic level would also have to account for the complex stimulus dependency of oscillatory behaviour observed in our study. It is therefore highly probable that rhythmicity is already present in the activity afferent to the recorded neuron.

Several hypotheses arise regarding the possible extrinsic sources of periodicity. One possibility is to consider the cortex as the recipient of a rhythm generated in the thalamus. Indeed, we observed oscillatory activity in the visual responses of certain thalamo-cortical fibres that matched the dominant frequency of cortical neurons. It has been shown *in vitro* that relay cells of the lateral geniculate nucleus (LGN) show periodic activity, and *in vivo* that the thalamo-cortical pathway is involved in the propagation of spindle and δ-waves (from thalamus to cortex) while the slow (< 1 Hz) oscillations follow the inverse stream (review in Steriade, McCormick & Sejnowski, 1993). Using extra-

cellular recordings, Ghose & Freeman (1992) observed γ range oscillations in the visual responses of single cortical neurons, and in the spontaneous and visual activity of geniculate cells. Since these oscillations were stronger in the LGN, they proposed that, during spontaneous activity, the LGN feeds the cortex with a background oscillatory activity which is not effective enough to reach the spike initiation threshold in the cortical cell. Visual stimulation would favour the expression of the modulation at the suprathreshold level by adding a synaptic DC component. Although we observed thalamo-cortical fibres oscillating in the absence of visual stimulation, this model of Ghose & Freeman (1992) seems difficult to apply to our own findings for several reasons. First, one would expect that intracellular cortical recordings might reveal stable LGN-originating subthreshold oscillations during spontaneous activity of cortical cells, which is not the case. Second, the model predicts that stimuli that are efficient for the cortical cells will favour their oscillatory behaviour, because the DC component added by the stimulus will be more important. This is indeed the case in their results, but fails to account for ours, since we were unable to find a correlation between the strength of the oscillations and the amplitude of the responses. Moreover, the complex orientation dependency we observed in some cases (see Fig. 11) argues more in favour of a cortical origin of the low frequency rhythms we observed.

Another possibility is that the functional architecture of the visual cortex itself generates oscillations, even if its constitutive elements are not by themselves intrinsic oscillators. Such models have been formally described in the literature (Wilson & Cowan, 1972). Possible contributions of excitation and inhibition will be discussed later. The majority of our oscillatory cells fire in the bursting mode, which may seem at first glance paradoxical given the independence of visually evoked oscillations on intrinsic properties. Some insights might come from rodent cortex, where it has been shown that bursting cells are highly interconnected, thus forming a 'subnetwork' that might generate rhythmic patterns (Silva, Chagnac-Amitai & Connors, 1991), and propagate them to other cortical cells. This raises the possibility that, at the collective level, voltage-dependent properties might be determinant in the setting of the rhythm, although the participation of each neuron might be negligible. Thus expression of certain temporal specificities in a densely connected excitatory network might lead to oscillatory resonance at a given frequency. Indeed, 'resonant properties' that have been reported for cortical pyramidal cells *in vitro* are below 25 Hz (Gutfreund *et al.* 1995). However, this interpretation should be taken with great caution because most of the data in the literature concerning laminar distribution of the firing modes in the visual cortex come from experiments made in slices of rodent cortex, and may not apply to feline cortex *in vivo*: in the motor cortex, bursting neurons are encountered at cortical depths between 900 and 1300 μm (Baranyi *et al.* 1993) and in the visual cortex, layer V pyramidal cells do show extensive axonal and dendritic arbours in infragranular layers (Martin & Whitteridge, 1984). The 'chattering' cells that could participate in the generation of higher rhythms have been recently reported to form a subclass of layer II–III pyramidal cells (Gray & McCormick, 1996).

Our results show that in most cases, the periodic events were depolarizing, even though they could be riding on a slower depolarizing or hyperpolarizing wave. Hyper-polarizing the membrane potential with a DC current led in all but one case to an increase in the amplitude of the depolarizing events, which pleads in favour of a dominant non-NMDA component, although because of space-clamp problems the involvement of NMDA responses cannot be fully characterized. Such an excitatory response profile seems to exclude architectures like Wilson–Cowan oscillators, formed by pairs of reciprocally connected excitatory and inhibitory interneurons (Wilson & Cowan, 1972), a schema that has been applied in a number of studies of synchronization of oscillatory activity (König & Schillen, 1991). However, we observed in two cases inhibitory synaptic potentials alternating with excitatory ones in response to a moving bar, with an approximate 45 deg phase, that did not depend on the direction of the stimulus, and consequently could not be explained by the spatial structure of the receptive field. This pattern was reminiscent of the classical EPSP–IPSP sequence following thalamic afferent stimulation (Douglas & Martin, 1991) and thus raises the possibility that oscillations observed in these two cells stemmed from synchronized thalamic discharge. We never observed rhythmic IPSPs in the absence of EPSPs.

Related data come from the group of Ferster (Ferster, 1986; Jagadeesh *et al.* 1992) and are based on a specific method for dissociating EPSPs from IPSPs in the visual response during intracellular recordings *in vivo*. The strategy was to evoke EPSPs and IPSPs following electrical stimulation of the LGN at fixed latency, and to assess their respective contribution by the injection of intracellular currents in order to polarize the cell close to the reversal potential of each synaptic component. The main assumptions were that: (1) EPSPs and IPSPs were temporally out of phase during the response to LGN stimulation, so that at any time delay after the electric shock the membrane potential reflected two non-interacting populations of PSPs, thus ruling out that the observed waveform was the net effect of a (possibly non-linear) combination; and (2) the current values necessary to abolish a PSP of a given type were the same for electrical and visual stimulation. This last hypothesis might be more debatable since visual processing could involve far more corticocortical connections, possibly characterized by a different set of electrotonic parameters than that recruited during the electrical stimulation of the LGN. In other words, there is no reason to believe *a priori* that the set of synapses activated by an LGN electrical shock might constitute a probe representative of the visually activated synapses. The

results obtained by this method were twofold: in an early study using sharp electrodes (Ferster, 1986), rhythmic IPSPs were reported in both simple and complex cells. A later study from the same laboratory, based on whole-cell recordings, put emphasis on EPSPs occurring at 40 Hz in response to a moving light bar. This effect was more pronounced in complex cells. However, the presented data did not fully support the assumptions of the method since a strong 40 Hz component was still observed when the cell was depolarized at a membrane potential level at which electrically evoked EPSPs were suppressed (Fig. 3 in Jagadeesh *et al.* 1992).

In summary, from the work of Jagadeesh *et al.* (1992) as well as our own, it appears that a clear-cut separation of excitation and inhibition is difficult in the absence of pharmacological techniques (but see Shulz *et al.* 1993). Furthermore determination in current clamp and voltage clamp of the potential for which reversal of visual PSCs or PSPs is observed should be taken with caution, because of space-clamp problems. However, our data document for the first time favourable cases, where events dominated by excitation can be identified. This is the case when the extrapolated reversal potential of the PSPs and PSCs is close to 0 mV (e.g. Fig. 6), or when EPSCs and IPSCs are out of phase (Fig. 7).

Possible functions of oscillatory activity

The functional significance of oscillatory activity is still an open matter for discussion. While it is for some authors a tool for promoting synchronized activity in cell assemblies (Engel *et al.* 1990), it has been described as purely epiphenomenal by others (Ghose & Freeman, 1992). According to the first schema, a given stimulus will activate a constellation of feature detectors in different cortical modules, responding to different dimensions of the stimulus. The working hypothesis is that the rhythmicity of response of each detector should favour synchronization, resulting in the binding of specific members of the initial assembly. Several studies have established that long-range synchronization occurs preferentially between cells coding for similar orientation when they are stimulated with their optimal stimulus (Ts'o *et al.* 1986; Gray *et al.* 1989). Therefore two strong predictions can be made concerning the instrumental role of oscillatory activity binding: (1) responses of the feature detectors should be oscillatory for their optimal stimulus; and (2) cortical domains coding values different from that contained in the stimulus should not oscillate. We have shown here that there is no correlation between the amplitude of the neuronal response and the strength of the oscillation, which means that cortical cells do not tend to oscillate more in response to their optimal feature, whereas they could strongly oscillate for non-optimal stimuli. In the theoretical framework sketched above, this would lead to erroneous synchronization. This simplistic reasoning is meant to pin down the weakness of a synchronization-by-oscillation model and pleads for a more comprehensive approach.

According to our data, oscillations at the single cell level induced by visual stimulation are not limited to the γ range, and appeared more as the signature of a working circuit than as a tool for temporal binding. Recently, König, Engel, Roelfsema & Singer (1995) have shown evidence in favour of a phase separation between circuits coding different orientations. Ideally, this would allow the orientation networks to avoid synchronization in the case of oscillatory pattern evoked by non-optimal orientation, such as those we have observed. Clearly, more experiments are needed to understand the origins of these rhythms and the relationships between the different frequencies evoked by visual stimulation. More theoretical work is also necessary in order to fully understand the contribution of the dynamics of single units to synchronization, for example by assessing the speed of synchronization with different types of neural activity (oscillatory, Poissonian and chaotic).

One of the main implications of our intracellular study is that presynaptic activity in oscillating cells is organized in 'packets' of spikes: the fast rise time of composite synaptic events observed during visual responses probably originates from many converging active fibres, showing a high degree of synchronization. Whatever the role of oscillations, synchronization of neuronal activity remains a very attractive candidate for the integration or binding of widespread activity. Indeed there are many reports of synchronized responses in the visual cortex independently of their oscillatory character (for example: Ts'o *et al.* 1986; Toyama, 1988). The extent to which packets of locally synchronized spiking events mediate non-periodic activity is the subject of future investigation.

Alonso, A. & Klink, R. (1993). Differential electroresponsiveness of stellate and pyramidal-like cells of medial entorhinal cortex layer II. *Journal of Neurophysiology* **70**, 128–143.

Andersen, P. & Andersson, S. A. (1968). *Physiological Basis of the Alpha Rhythm.* Appleton Century Crofts, New York.

Baranyi, A., Szente, M. B. & Woody, C. D. (1993). Electrophysiological characterization of different types of neurons recorded *in vivo* in the motor cortex of the cat. I. Patterns of firing activity and synaptic responses. *Journal of Neurophysiology* **69**, 1850–1864.

Bringuier, V., Frégnac, Y., Debanne, D., Shulz, D. & Baranyi, A. (1992). Synaptic origin of rhythmic visually evoked activity in kitten area 17 neurons. *NeuroReport* **3**, 1065–1068.

Buzsaki, G., Horvath, Z., Urioste, R., Hetke, J. & Wise, K. (1992). High frequency network oscillation in the hippocampus. *Science* **256**, 1025–1027.

Cox, D. R. (1962). *Renewal Theory.* Methuen, London.

CREUTZFELDT, O. D., WATANABE, S. & LUX, H. D. (1966). Relations between EEG phenomena and potentials of single cortical cells. II. Spontaneous and convulsoid activity. *Electroencephalography and Clinical Neurophysiology* **20**, 19–37.

DEPPISCH, J., BAUER, H. U., SCHILLEN, T., KÖNIG, P., PAWELZIK, K. & GEISE, T. (1993). Alternating oscillatory and stochastic states in a network of spiking neurons. *Network* **4**, 243–257.

DOUGLAS, R. J. & MARTIN, K. A. C. (1991). A functional microcircuit for cat visual cortex. *Journal of Physiology* **440**, 735–769.

ECKHORN, R., BAUER, R., JORDAN, W., BROSCH, M., KRUSE, W., MUNK, M. & REITBOCK, H. J. (1988). Coherent oscillations: A mechanism of feature linking in the visual cortex? *Biological Cybernetics* **60**, 121–130.

ECKHORN, R., BAUER, R., JORDAN, W., EPPING, W. & ARNDT, M. (1987). Correlated activity and coding properties of neuron groups within vertical columns of the visual cortex: a multi-electrode study. *Neuroscience* **22**, S435.

ENGEL, A. K., KÖNIG, P., GRAY, C. M. & SINGER, W. (1990). Stimulus-dependent neuronal oscillations in cat visual cortex: Inter-columnar interaction as determined by cross-correlation analysis. *European Journal of Neuroscience* **2**, 588–606.

FERSTER, D. (1986). Orientation selectivity of synaptic potentials in neurons of cat primary visual cortex. *Journal of Neuroscience* **6**, 1284–1301.

FREEMAN, W. J. & SKARDA, C. A. (1985). Spatial EEG patterns, non-linear dynamics and perception: the neo-Sherringtonian view. *Brain Research Review* **18**, 147–175.

FRÉGNAC, Y. (1982). Développement de la sélectivité neuronale dans le cortex visuel primaire du chat. Doctorat d'Etat es-Sciences Naturelles, Paris VI.

FRÉGNAC, Y. (1991). How many cycles make an oscillation? In *Representations of Vision: Trends and Tacit Assumptions in Vision Research*, ed. GOREA, A., FRÉGNAC, Y., KAPOULA, Z. & FINLAY, J., pp. 97–109. Cambridge University Press, Cambridge.

FRÉGNAC, Y., SHULZ, D., THORPE, S. & BIENENSTOCK, E. (1992). Cellular analogs of visual cortical epigenesis: I. Plasticity of orientation selectivity. *Journal of Neuroscience* **12**, 1280–1300.

GALLANT, J. (1986). Three construction algorithms for network training. *Proceedings of the 8th Annual Conference of the Cognitive Science Society*, 652–660.

GHOSE, G. M. & FREEMAN, R. D. (1992). Oscillatory discharge in the visual system: does it have a functional role? *Journal of Neurophysiology* **68**, 1558–1574.

GRAY, C. M., ENGEL, A. K., KÖNIG, P. & SINGER, W. (1990). Stimulus-dependent neuronal oscillations in cat visual cortex. Receptive field properties and feature dependence. *European Journal of Neuroscience* **2**, 607–619.

GRAY, C. M., KÖNIG, P., ENGEL, A. K. & SINGER, W. (1989). Oscillatory responses in cat visual cortex exhibit inter-columnar synchronization which reflects global stimulus properties. *Nature* **338**, 334–337.

GRAY, M. & MCCORMICK, D. A. (1996). Chattering cells: superficial pyramidal neurons contributing to the generation of synchronous oscillations in the visual cortex. *Science* **274**, 109–113.

GUTFREUND, Y., YAROM, Y. & SEGEV, I. (1995). Subthreshold oscillations and resonant frequency in guinea-pig cortical neurons: physiology and modelling. *Journal of Physiology* **483**, 621–640.

JAGADEESH, B., GRAY, C. M. & FERSTER, D. (1992). Visually evoked oscillations of membrane potential in cells of cat visual cortex. *Science* **257**, 552–554.

KÖNIG, P., ENGEL, A. K., ROELFSEMA, P. & SINGER, W. (1995). How precise is neuronal synchronization? *Neural Computation* **7**, 469–485.

KÖNIG, P. & SCHILLEN, T. B. (1991). Stimulus dependent-assembly formation of oscillatory responses: I. Synchronization. *Neural Computation* **3**, 155–166.

KOPELL, N. & LE MASSON, G. (1994). Rhythmogenesis, amplitude modulation, and multiplexing in a cortical architecture. *Proceedings of the National Academy of Sciences of the USA* **91**, 10586–10590.

MCCORMICK, D. A., CONNORS, B. W., LIGHTHALL, J. W. & PRINCE, D. A. (1985). Comparative electrophysiology of pyramidal and sparsely spiny stellate neurons of the neocortex. *Journal of Neurophysiology* **54**, 782–806.

MCCORMICK, D. A. & GRAY, C. M. (1995). Physiologically identified cell groups have distinct receptive field and morphological properties in cat striate cortex. *Society for Neuroscience Abstracts* **21**, 1506, 592.6.

MARKRAM, H. & SAKMANN, B. (1994). Calcium transients in dendrites of neocortical neurons evoked by single subthreshold excitatory postsynaptic potentials via low-voltage-activated calcium channels. *Proceedings of the National Academy of Sciences of the USA* **91**, 5207–5211.

MARTIN, K. A. C. & WHITTERIDGE, D. (1984). Form, function and intracortical projections of spiny neurones in the striate visual cortex of the cat. *Journal of Physiology* **353**, 463–504.

SCHILLEN, T. B., KÖNIG, P., ENGEL, A. K. & SINGER, W. (1992). Development of oscillatory neuronal activity in the visual cortex of the cat. *European Journal of Neuroscience* suppl. 5, 165.

SHULZ, D., BRINGUIER, V. & FRÉGNAC, Y. (1993). Complex-like structure of simple visual cortical receptive fields is masked by $GABA_A$ intracortical inhibition. *Society for Neuroscience Abstracts* **19**, 638.

SILVA, L. R., CHAGNAC-AMITAI, Y. & CONNORS, B. W. (1991). Intrinsic oscillations of neocortex generated by layer V pyramidal neurons. *Science* **251**, 432–435.

STERIADE, M., MCCORMICK, D. & SEJNOWSKI, T. J. (1993). The sleeping and aroused brain: Thalamocortical oscillations in neurons and networks. *Science* **262**, 679–685.

STUART, G. J. & SAKMANN, B. (1994). Active propagation of somatic action potentials into neocortical pyramidal cell dendrites. *Nature* **367**, 69–72.

TOVEE, M. J. & ROLLS, E. T. (1992). Oscillatory activity is not evident in the primate temporal visual cortex with static stimuli. *NeuroReport* **3**, 369–372.

TOYAMA, K. (1988). Functional connections of the visual cortex studied by cross-correlation techniques. In *Neurobiology of Neocortex*, ed. RAKIC, P. & SINGER, W., pp. 203–217. W. J. Wiley and Sons, New York.

TS'O, D. Y., GILBERT, C. D. & WIESEL, T. N. (1986). Relationships between horizontal interactions and functional architecture in cat striate cortex as revealed by cross-correlation analysis. *Journal of Neuroscience* **6**, 1160–1170.

VON KROSIGK, M., BAL, T. & MCCORMICK, D. A. (1993). Cellular mechanisms of a synchronized oscillation in the thalamus. *Science* **261**, 361–364.

WILSON, H. R. & COWAN, J. D. (1972). Excitatory and inhibitory interactions in localized populations of model neurons. *Biophysical Journal* **12**, 1–24.

YOUNG, M. P., TANAKA, K. & YAMANE, S. (1992). On oscillating responses in the visual cortex of the monkey. *Journal of Neurophysiology* **67**, 1464–1474.

Acknowledgements

We wish to thank Dr L. Borg-Graham and C. Monier who devised the *in vivo* patch technique in our laboratory, Dr C. Linster for suggesting and running the analysis using the pocket algorithm, G. Sadoc for software development, and Dr K. Grant for help with the English. We are grateful to Drs E. Ahissar, L. Borg-Graham, R. Freeman, G. Ghose and W. Singer for valuable comments on an earlier version of the manuscript. This work was supported by grants to Y.F. from the Human Frontier Science Programme (RG 69/93 B) and the Ministère de la Recherche et de la Technologie (MRT; 91C0953). A.B. was supported by CNRS, and V.B. by scholarships from MRT and Fondation Fouassier.

Authors' present addresses

A. Baranyi: Attila Joszef University of Sciences, Szeged, Hungary.

V. Bringuier: Instituto das Ciencias Biologicas, UFMG, Belo Horizonte, Brazil.

D. Debanne: Unité de Neurocybernétique cellulaire, CNRS, 1309 Marseille, France.

Received 22 August 1996; accepted 17 January 1997.